Supplementary Information for

Cucurbituril-Activated Photoreaction of Dithienylethene for Controllable Targeted Lysosomal Imaging and Anti-Counterfeiting

Guoxing Liu,[a,b] Xiufang Xu,[a] Xianyin Dai,[a] Chunhui Jiang,[a] Yu Zhou,[a] Lei Lu[c] and Yu Liu[a]*

[a]College of Chemistry, State Key Laboratory of Elemento-Organic Chemistry, Nankai University, Tianjin 300071, P. R. China

[b]College of Science, Henan Agricultural University, Zhengzhou, Henan 450002, P. R. China

[c]College of Information Science and Engineering, Henan University of Technology, Zhengzhou 450001, P. R. China

*E-mail: yuliu@nankai.edu.cn

Table of Contents

Materials and methods

Instruments and methods. All manipulations were carried out under an argon atmosphere by using standard Schlenk techniques. THF was distilled under argon atmosphere from sodium-benzophenone. All starting materials were obtained commercially as analytical-grade and used without further purification. NMR spectra were recorded on a BrukerAV400 spectrometer at 25 °C. High resolution mass (HR-MS) spectra were measured in the MALDI or ESI mode. TEM images were acquired using a Tecnai 20 transmission electron microscope operating at an accelerating voltage of 200 kV. The sample for TEM measurements was prepared by dropping a sample solution (2.0×10^{-5} M in water) onto a copper grid and was then air dried. The hydrodynamic diameter (D_h) was determined by DLS experiments at 25 °C, and solution samples（2.0×10^{-5} M in water） were examined on Malvern Zetasizer Nano ZS90. Irradiation experiments ($\lambda = 405$ nm and >490 nm) was carried out using a CEL-HXF300 20V 300W xenon lamp (Beijing China Education Au-light Co. Ltd., China) with a 25% attenuating filter and a band-pass optical filter for 405 nm light and with a 25% attenuating filter and cutoff optical filter for >490 nm light, respectively. The exact optical power densities of 405 nm and >490 nm light in irradiation experiments were determined to be 12.72 mw/cm^2 and 88.3 mw/cm^2, respectively, using optical power meter (CEL-NP2000-2A). Photocontrolled target lysosomal imaging experiments were performed using light sources of the laser confocal imager itself, which are near ultraviolet pulse laser (405 nm, 3 mW) and red HeNe pulse laser (633 nm, 10 mW), respectively.

Spectroscopy measurements. UV-vis absorption spectra were measured in a quartz cell (light path, 10mm) on a Shimadzu UV-2401PC spectrophotometer equipped with a Thermo HAAKE-SC100 temperature controller. Steady-state fluorescence spectra of DTE-MPBT, DTE-MPBT⊂CB[8] and solid-state DTE-MPBT⊂CB[8] were recorded in a conventional quartz cell (light path, 10 mm) on HITACHI F-7000 FL. Absolute quantum yield of liquid and solid-state DTE-MPBT⊂CB[8] was obtained by Absolute PL Quantum Yield Spectrometer C11347 (Hamamatsu, Japan). Hamamatsu Quantaurus-Tau spectrometer was used to measure fluorescence lifetime.

Cytotoxicity experiments. Human lung adenocarcinoma cells (A549 cells) were incubated in Dulbecco's modified Eagle's medium (DMEM). The medium was supplemented with 10% fetal bovine serum. A549 cells were seeded in 96-well plates (5×10^4 cell mL^{-1},0.1 mL per well) for 24 h at 37 ℃ in 5% CO_2. Then the cells were incubated with DTE-MPBT⊂CB[8] ([DTE-MPBT] = [CB[8]] =2×10^{-5} M) for 24 h. The relative cellular viability was determined by the MTT assay.

Confocal fluorescence images. A549 cells were seeded in confocal dish (5×10^4 cell mL^{-1}, 1 mL) for 24 h at 37℃ in 5% CO_2. The cells were incubated with the corresponding solution for 4 h. Then the medium was removed, and the cells were washed with phosphate buffer solution for three time and fixed with 4% paraformaldehyde for 15 min. Finally, the cells were subjected to observation by a confocal laser scanning microscope. The variation and reversibility of confocal fluorescence images of A549 cells co-stained with DTE-MPBT⊂CB[8] in the same region were irradiated using alternate 405 nm and 633 nm laser.

Synthetic procedures of all new compounds

*Synthesis of **3***

In a 100 mL two-necked, round-bottom flask equipped with a magnetic stirrer was placed a mixture of **1**[1] (0.29 g, 0.50 mmol) and **2** (0.15 g, 1.20 mmol), and then acetic acid (10 mL) was added. The reaction mixture was refluxed for 12 h. The resulting mixture was cooled to ambient temperature, and added into ice water. After that, Na_2CO_3(s) was added to neutralize acetic acid. Subsequently, the residue was extracted by dichloromethane, and dried over anhydrous Na_2SO_4. The solvent was removed under vacuum, and the residue was purified on a silica gel column using petroleum ether / dichloromethane (1:3) as the eluent to obtain compound **3** as a light blue solid. Yield: 0.34 g, 86%. ^{1}H NMR (400 MHz, $CDCl_3$) δ ppm = 8.12 (d, J = 8.4 Hz, 2H), 8.09 (d, J = 8.0 Hz, 2H), 7.92 (d, J = 7.2 Hz, 2H), 7.67 (d, J = 8.4 Hz, 4H), 7.51 (t, J = 8.4, 2H), 7.41 (t, J = 8.8, 4H), 2.02 (s, 6H). ^{13}C NMR (100 MHz, $CDCl_3$) δ ppm = 167.13, 154.14, 142.33, 141.23, 135.57, 135.00, 132.91, 128.16, 126.46, 126.09, 125.90, 125.33, 123.27, 123.22, 121.64, 14.72. HRMS (MALDI) for $C_{41}H_{25}F_6N_2S_4^+$ [M+H$^+$]: calcd. 787.0805, found 787.0803.

Synthesis of DTE-MPBT

A solution of **3** (0.39 g, 0.5 mmol) and 3 mL CH_3I was placed in 10 mL pressure tube, and the mixture was heated at 110 ℃ for 24 h and cooled to room temperature. The solvent was removed under reduced pressure, and subsequent ion exchange with tetrabutyl ammonium chloride was performed to obtain photoswitchable compound DTE-MPBT. Yield: 0.40 g, 90%. ^{1}H NMR (400 MHz, DMSO) δ ppm = 8.57 (d, J = 8.0 Hz, 2H), 8.44 (d, J = 8.4 Hz, 2H), 8.08 (d, J = 8.4 Hz, 2H), 8.05 (d, J = 16.4 Hz, 4H), 8.01 (d, J = 7.2 Hz, 4H), 7.93 (d, J = 8.0 Hz, 2H), 7.90 (s, 2H), 4.28 (s, 6H), 2.06 (s, 6H). ^{13}C NMR (100 MHz, DMSO) δ ppm = 174.52, 144.74, 143.46, 140.80, 138.27, 132.55, 130.96, 130.67, 129.69, 127.10, 126.49, 126.22, 125.61, 125.43, 118.72, 39.10 (s), 15.26 (s). HRMS (MALDI) for $C_{43}H_{29}F_6N_2S_4^+$ [M-HCl-Cl$^-$]: calcd. 815.1112, found 815.1099.

*Synthesis of **5***

Compound **5** was prepared from **2** and **4**, and the synthesis procedure was similar to the synthesis of **3**. Yield: 0.14g, 88%. ^{1}H NMR (600 MHz, $CDCl_3$) δ ppm = 8.18 (d, J = 8.4 Hz, 1H), 8.15 (d, J = 8.4 Hz, 2H), 7.91 (d, J = 8.4 Hz, 1H), 7.68 (d, J = 8.4 Hz, 2H), 7.54 (t, J = 7.8 Hz, 1H), 7.43 (t, J = 7.8 Hz, 1H), 7.25 (d, J = 3.6 Hz, 1H), 6.78 (d, J = 3.6 Hz, 1H), 2.54 (s, 3H). ^{13}C NMR (100 MHz, $CDCl_3$) δ ppm = 167.68, 140.90, 140.75, 137.27, 134.77, 131.66, 128.07, 126.56, 126.42, 125.65, 125.21, 124.02, 123.01, 121.59, 15.55. HRMS (ESI) for $C_{18}H_{14}NS_2^+$ [M + H$^+$]: calcd. 308.0562, found 308.0565.

Synthesis of T-MPBT

The synthesis procedure of T-MPBT was similar to the synthesis of DTE-MPBT. Yield: 0.17g, 93%. ^{1}H NMR (400 MHz, DMSO) δ ppm = 8.55 (d, J = 8.4 Hz, 1H), 8.42 (d, J = 8.4 Hz, 1H), 8.01 (t, J = 7.2 Hz, 1H), 7.98 (s, 4H), 7.90 (t, J = 7.2 Hz, 1H), 7.65 (d, J = 3.6 Hz, 1H), 6.96 (dd, J = 3.6, 1.2 Hz, 1H), 4.28 (s, 3H), 2.53 (s, 3H). ^{13}C NMR (400 MHz, DMSO) δ ppm = 142.96, 142.78, 139.37, 139.25, 131.95, 130.36, 130.01, 129.10, 128.13, 127.07, 126.02, 125.02, 123.83, 118.17, 38.63, 15.75. HRMS (ESI) for $C_{19}H_{16}NS_2^+$ [M – Cl$^-$]: calcd. 322.0719, found 322.0721.

Supplementary Scheme and Figures

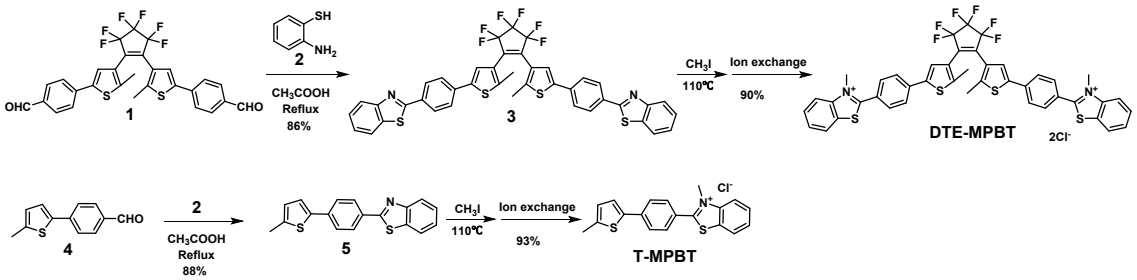

Scheme S1. The synthetic routes of DTE-MPBT and T-MPBT.

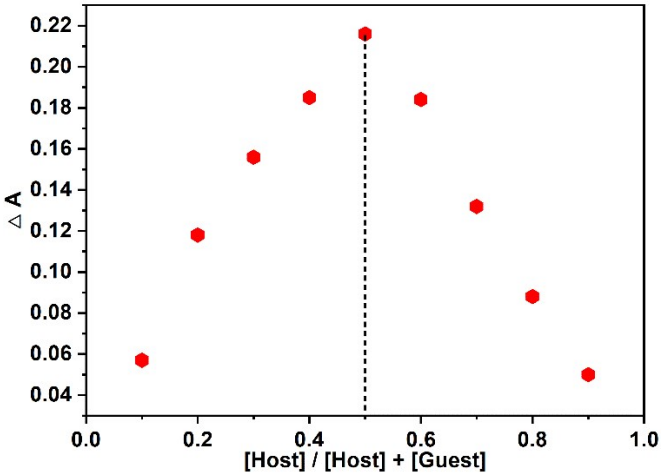

Figure S1. Host–guest binding stoichiometry experiment for guest DTE-MPBT and host CB[8]. Job plot for DTE-MPBT upon complexation with CB[8] in aqueous solution at 25 °C. Absorption changes recorded at 395 nm for DTE-MPBT. The sum of the total concentrations of hosts and guests is constant (2.0×10^{-5} M).

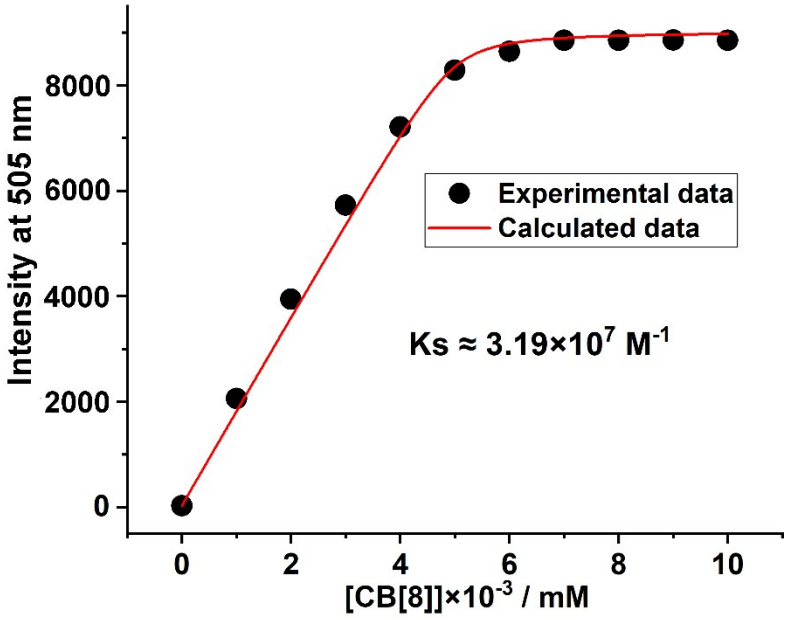

Figure S2. Nonlinear least-squares fit of the fluorescence intensity changes at 505 nm with continuous addition of CB[8] to determine the complex stability constant (K_S) as $3.19 \times 10^7\ M^{-1}$.

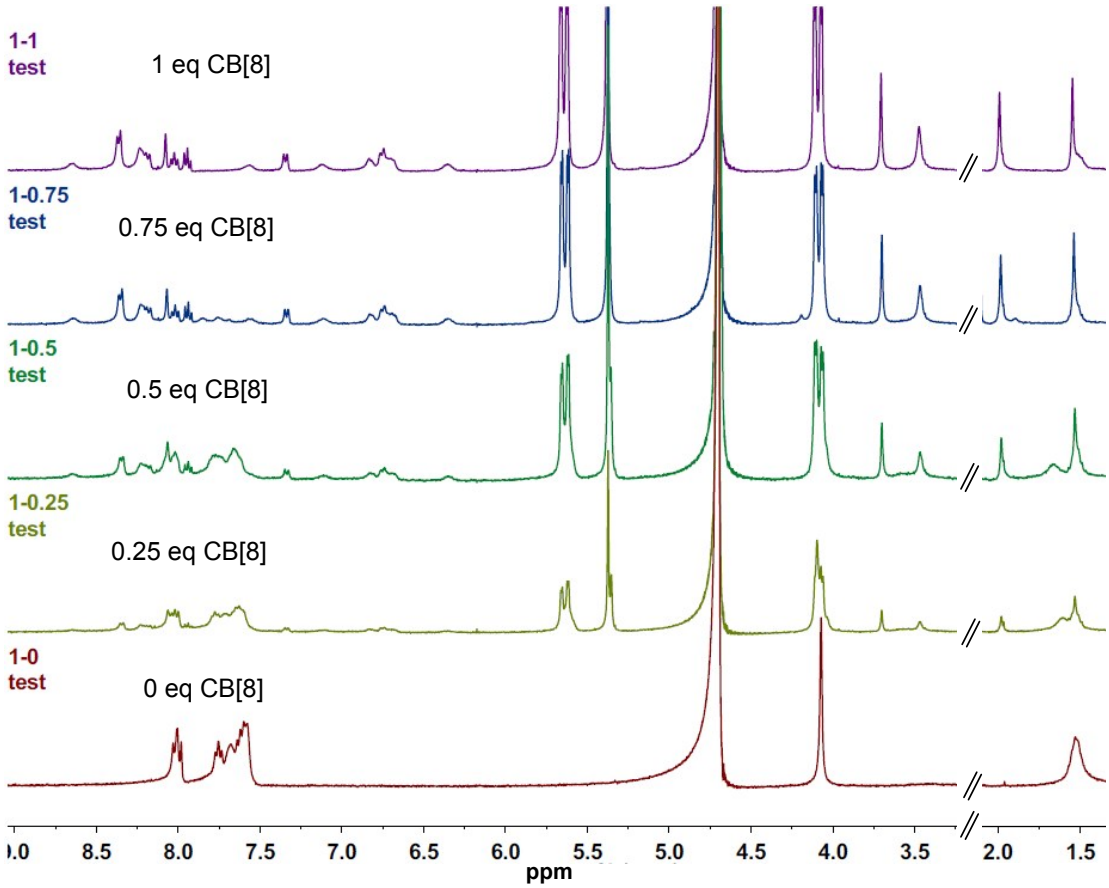

Figure S3. The variation of the ^1H NMR (400 MHz, D_2O) signals of DTE-MPBT upon continuous addition of CB[8] (0 eq, 0.25 eq, 0.5 eq, 0.75 eq and 1 eq).

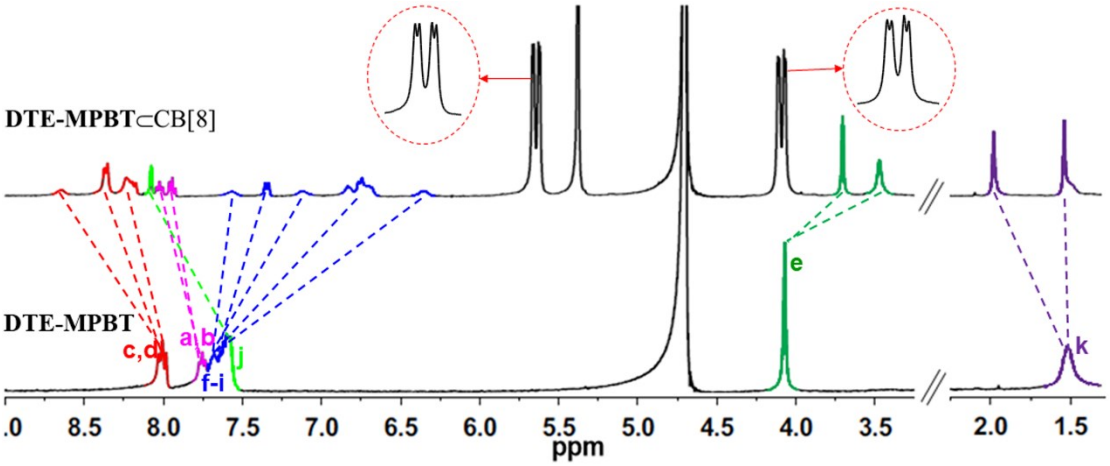

Figure S4. Partial ^{1}H NMR spectra of DTE-MPBT and DTE-MPBT⊂CB[8].

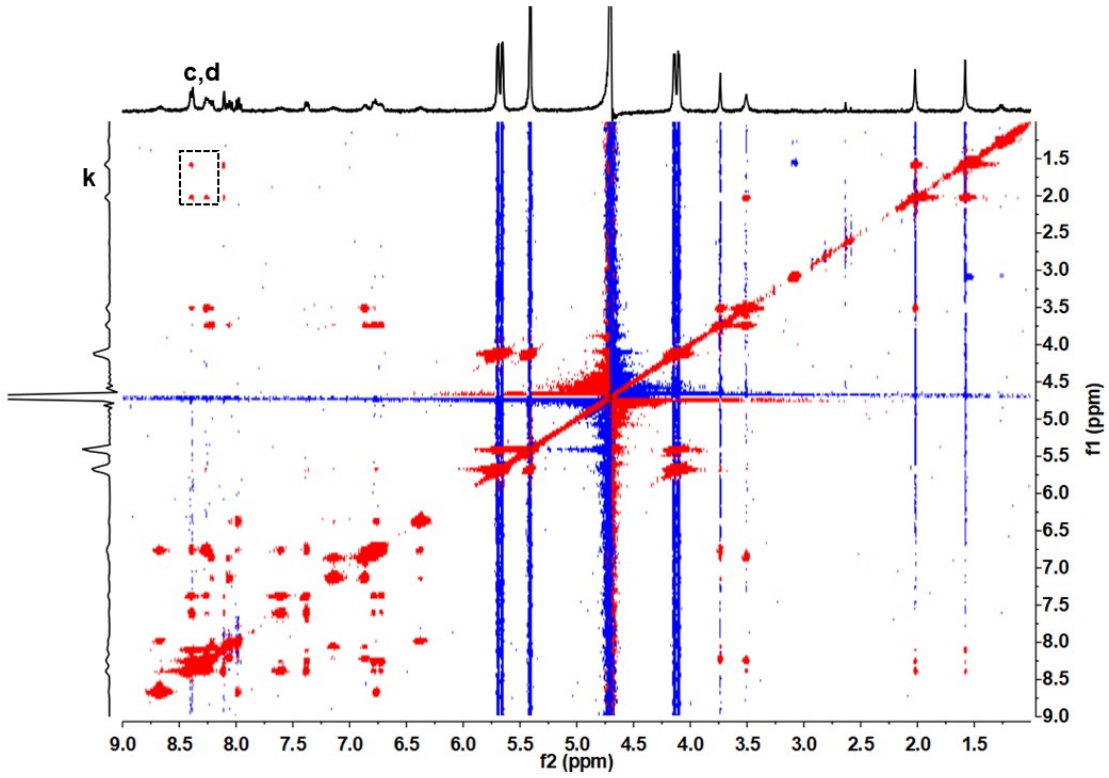

Figure S5. NOESY spectrum of assembly DTE-MPBT⊂CB[8] in D_2O at 25 ℃.

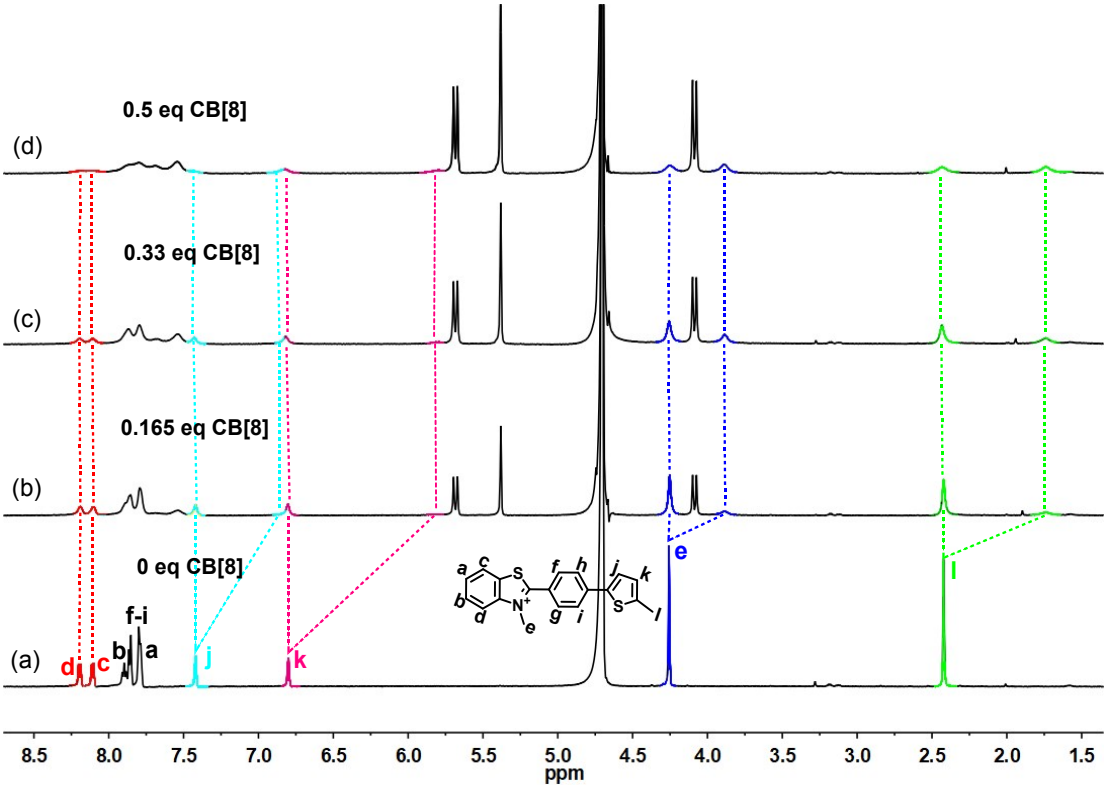

Figure S6. The variation of ^{1}H NMR (400 MHz, D_2O) signals of T-MPBT upon

continuous addition of CB[8] (0 eq, 0.165 eq, 0.33 eq and 0.5 eq).

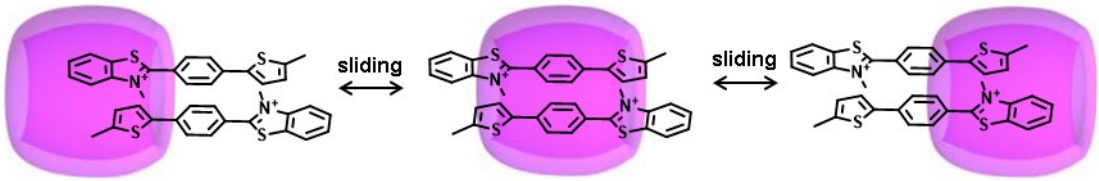

Figure S7. An ideal inclusion pattern of assembly T-MPBT⊂CB[8].

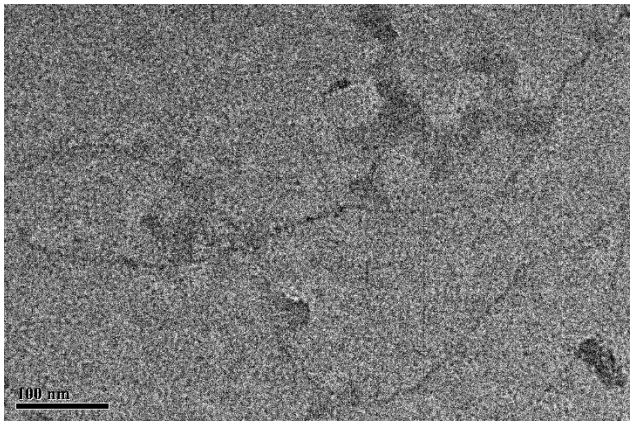

Figure S8. TEM images of DTE-MPBT⊂CB[8].

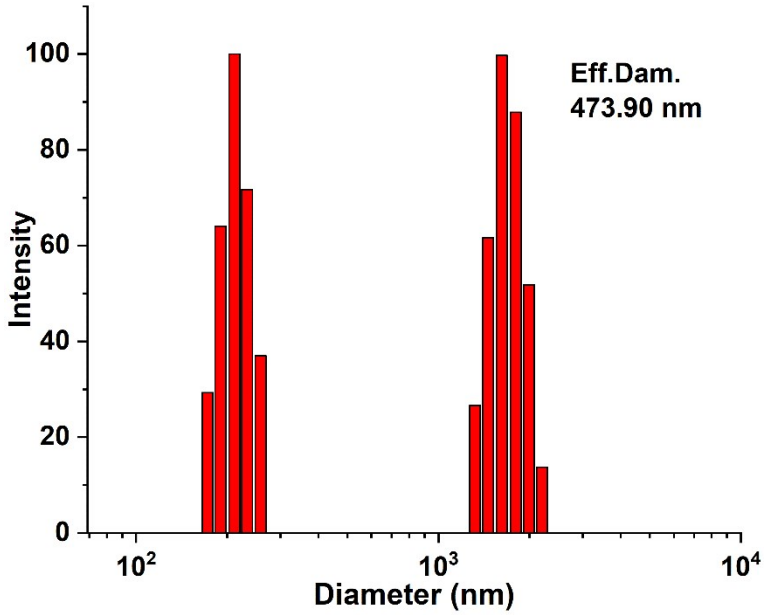

Figure S9. The DLS result of the DTE-MPBT⊂CB[8].

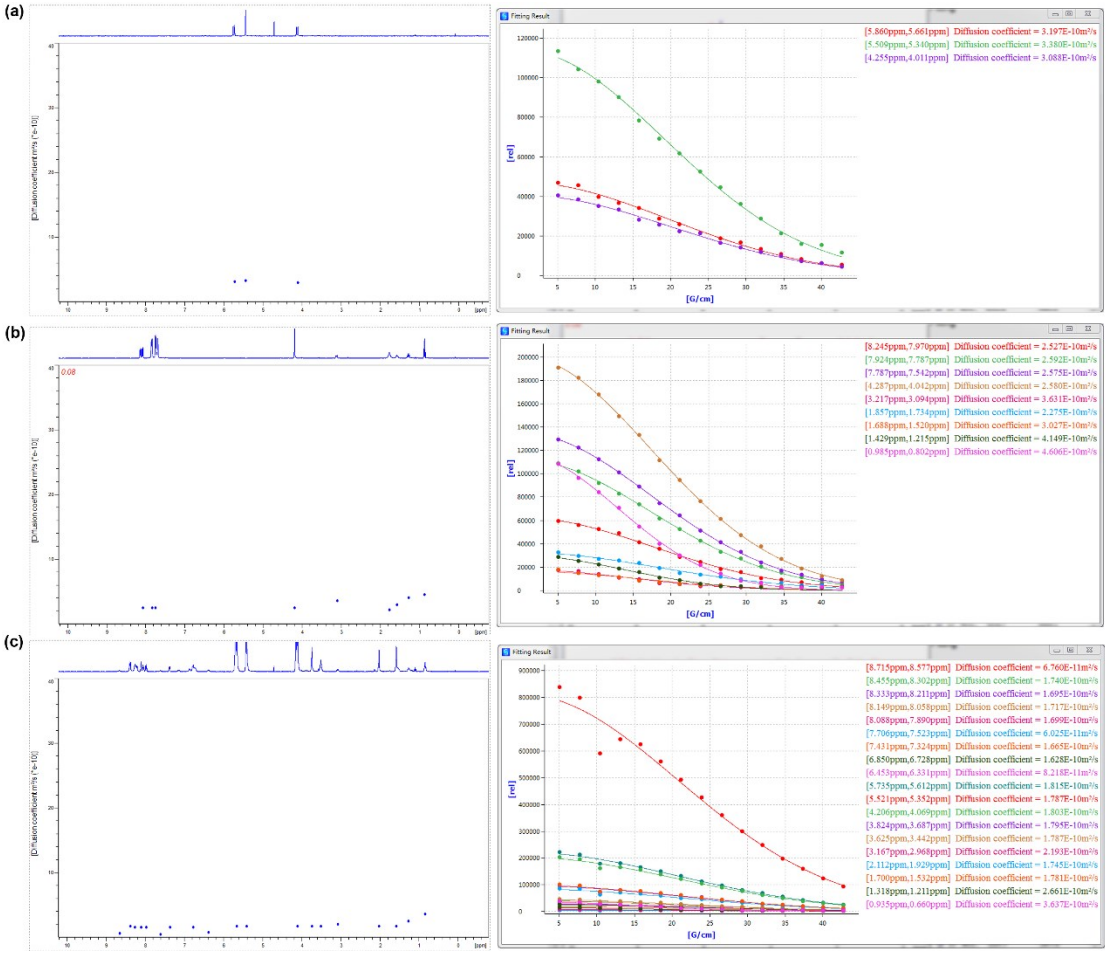

Figure S10. 2D DOSY spectrum (400 MHz, 298 K, D_2O). (a) Diffusion coefficient of CB[8] (0.1 mM). (b): Diffusion coefficient of DTE-MPBT (1.0 mM). (c) Diffusion coefficient of DTE-MPBT⊂CB[8] (1.0 mM).

Table S1. Diffusion coefficients (*D*) obtained from DOSY measurements

Complex	Diffusion coefficient ($m^2\ s^{-1}$)	$V_{complex}$ / $V_{CB[8]}$
CB[8]	3.22×10^{-10}	1
DTE-MPBT	3.11×10^{-10}	1.1
DTE-MPBT⊂CB[8]	1.55×10^{-10}	9.0

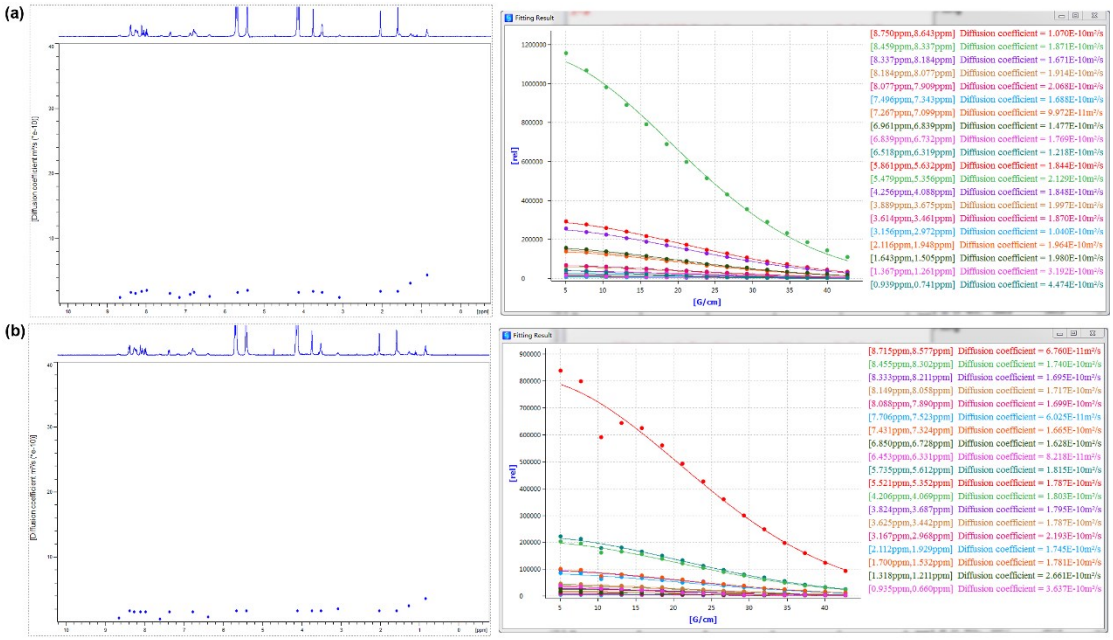

Figure S11. 2D DOSY spectrum (400 MHz, 298 K, D_2O). (a): Diffusion coefficient of DTE-MPBT⊂CB[8] (0.5 mM). (b): Diffusion coefficient of DTE-MPBT⊂CB[8] (1.0 mM).

Table S2. Diffusion coefficients (*D*) obtained from DOSY measurements

Complex	Concentration (mol/L)	Diffusion coefficient ($m^2\ s^{-1}$)
DTE-MPBT⊂CB[8]	0.5×10^{-3}	1.73×10^{-10}
DTE-MPBT⊂CB[8]	1.0×10^{-3}	1.55×10^{-10}

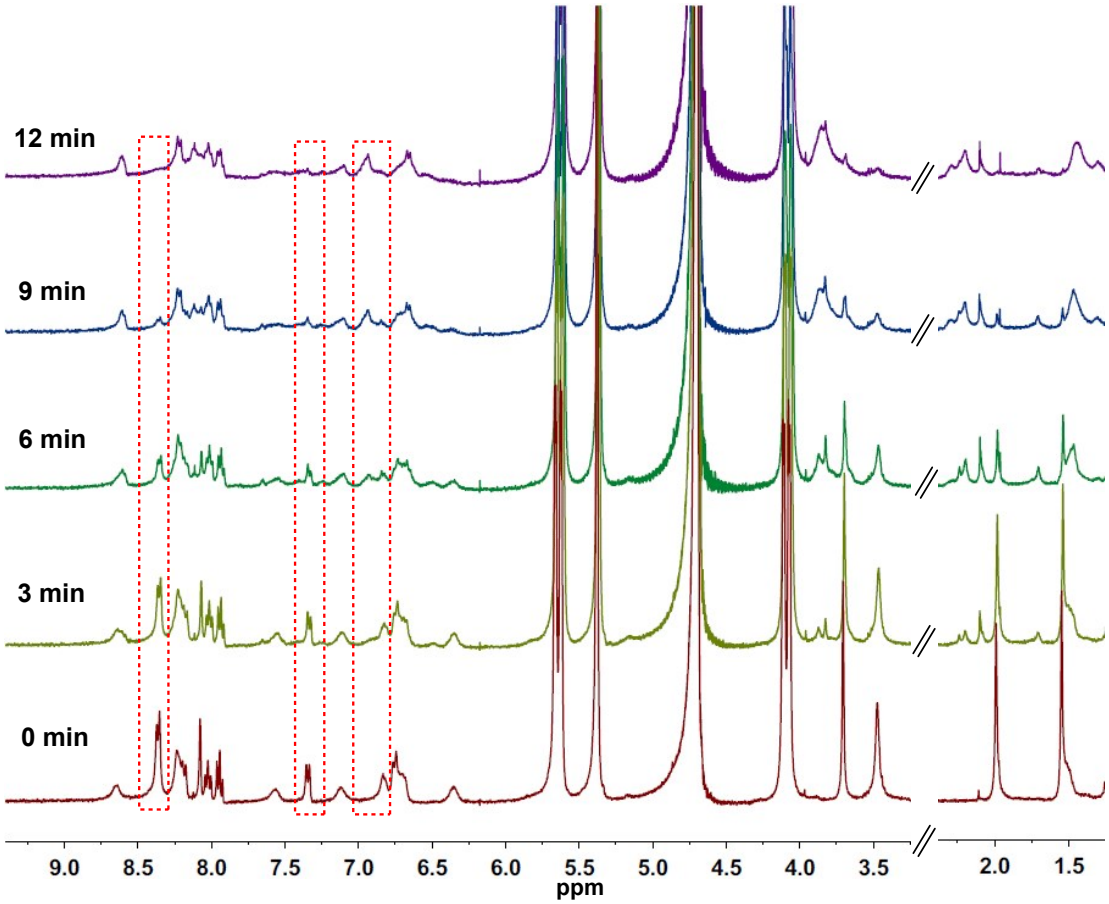

Figure S12. The variation of the ^{1}H NMR (400 MHz, D_2O) signals of DTE-MPBT⊂CB[8] upon 405 nm light irradiation. Photocyclization conversion yield is determined to be 95% through the calculation of nuclear magnetic integral area.

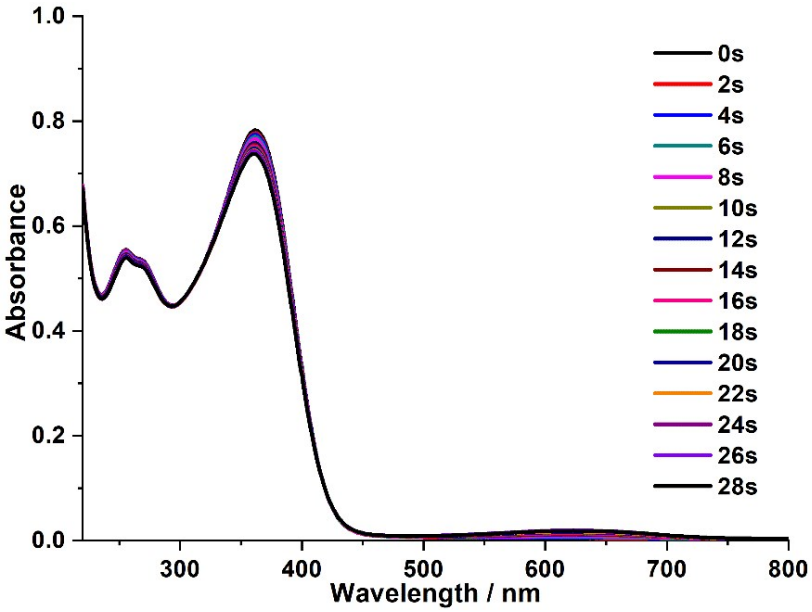

Figure S13. UV-vis absorption spectral changes of DTE-MPBT upon irradiation at 405

nm visible light for 28s.

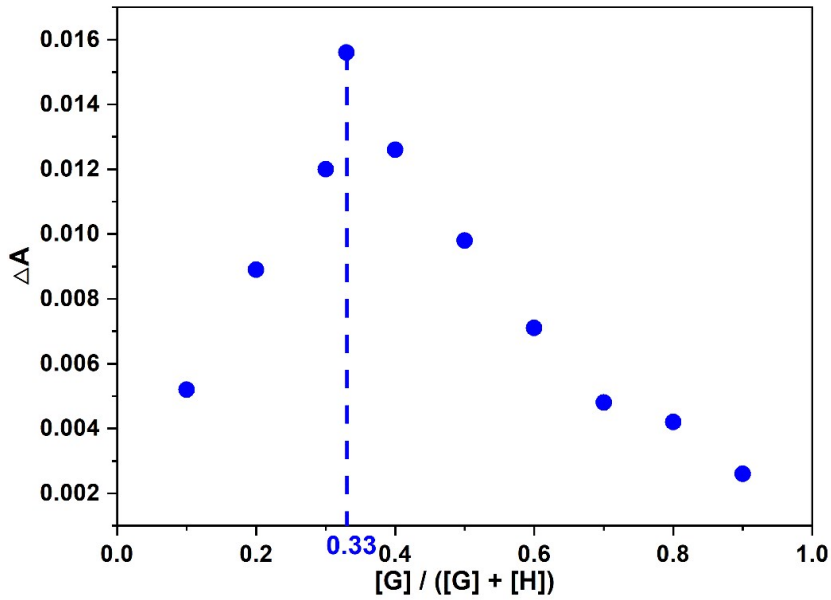

Figure S14. Host–guest binding stoichiometry experiment for guest DTE-MPBT and host CB[7]. Job plot for DTE-MPBT upon complexation with CB[7] in aqueous solution at 25 °C. Absorption changes recorded at 365 nm for DTE-MPBT. The sum of the total concentrations of hosts and guests is constant (2.0×10^{-5} M).

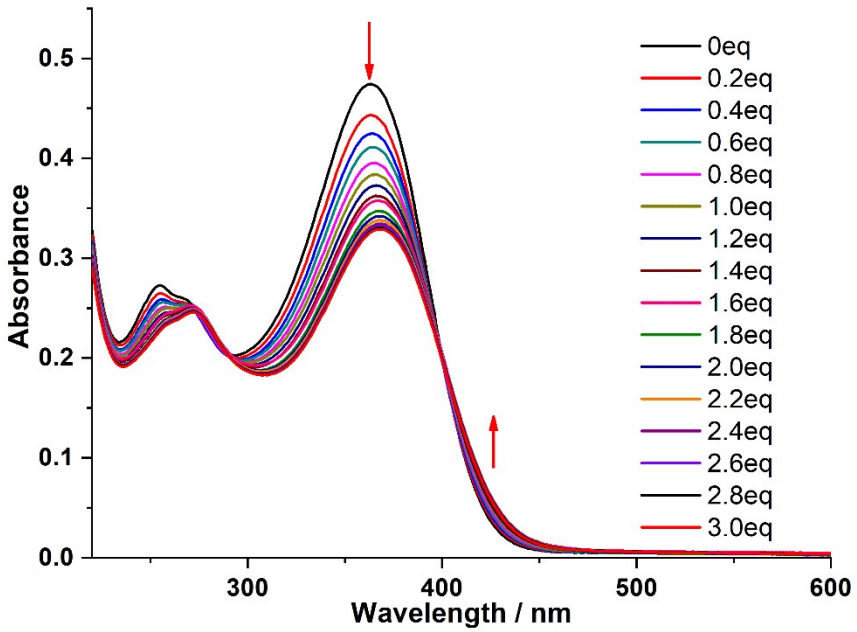

Figure S15. UV-vis absorption spectral change of DTE-MPBT (1.0×10^{-5} M) with sequential addition of 0 ～ 3 eq CB[7].

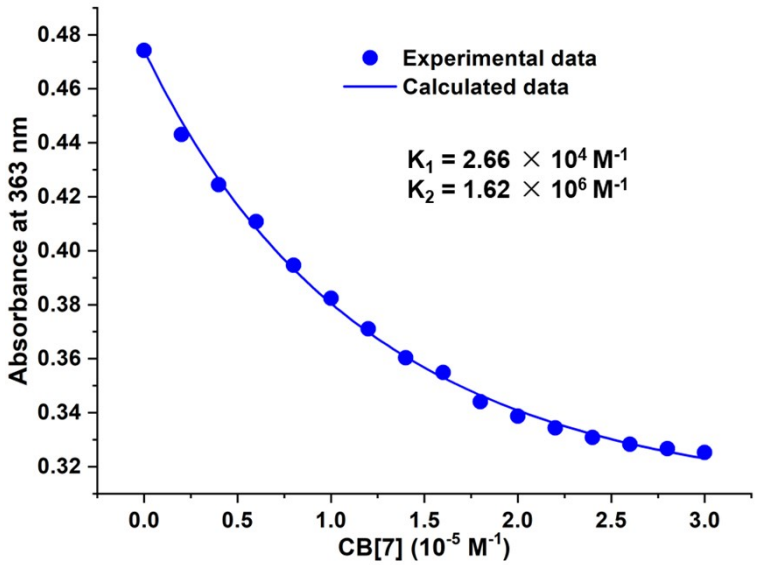

Figure S16. Nonlinear least-squares fit of the UV-vis absorbance change of DTE-MPBT at 363 nm with sequential addition of CB[7] to determine the complex stability constant (K_S) as 2.66×10^4 M^{-1} (K_1) and 1.62×10^6 M^{-1} (K_2).

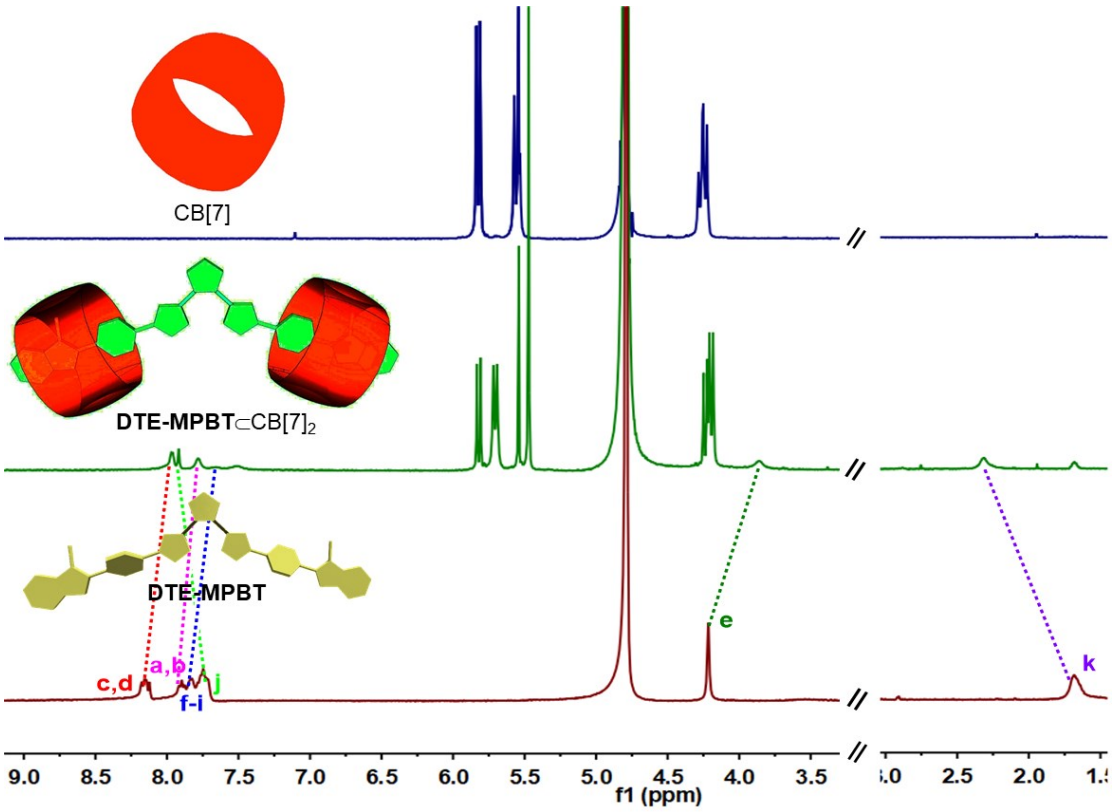

Figure S17. ^{1}H NMR (400 MHz, D_2O) spectra of DTE-MPBT, DTE-MPBT⊂CB[7]$_2$ and CB[7].

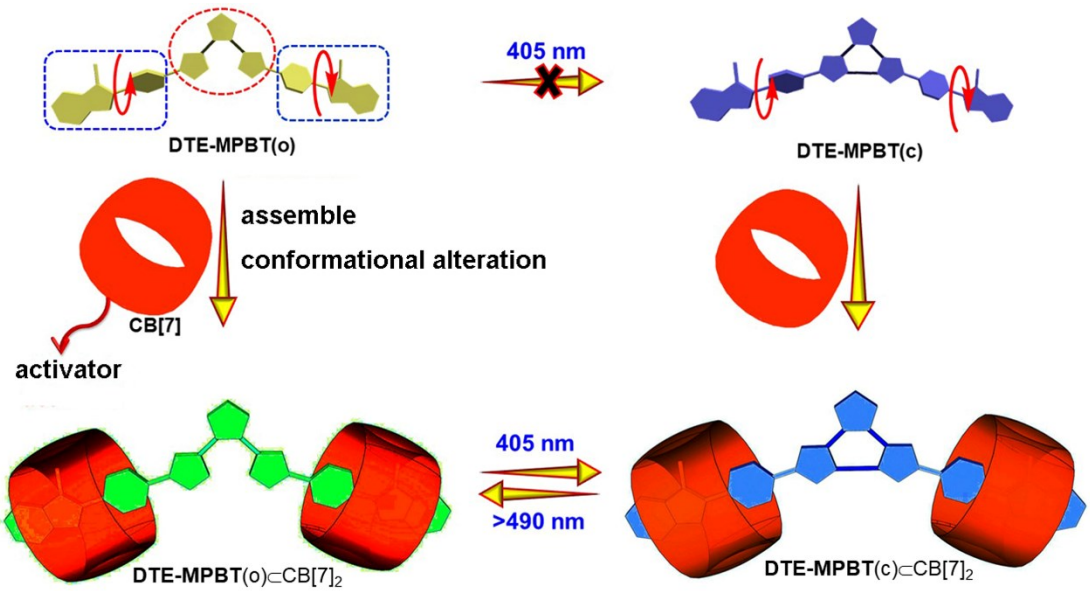

Figure S18. The proposed assembling pattern and assembly-activated photochromism of DTE-MPBT and CB[7].

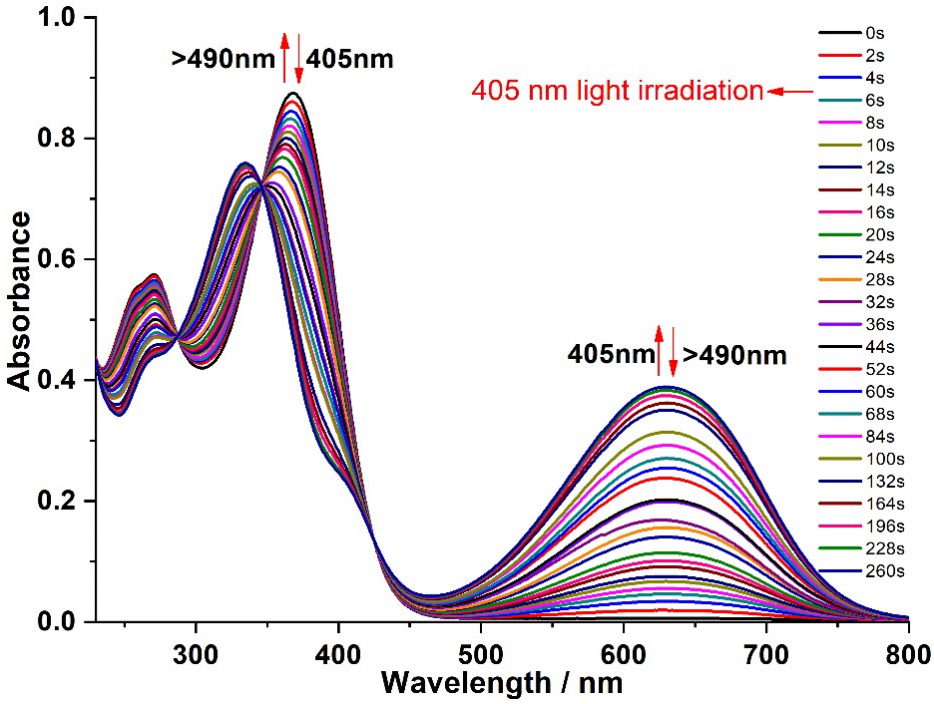

Figure S19. UV-vis absorption spectral change of DTE-MPBT⊂CB[7]$_2$ upon irradiation at alternative 405 nm and >490 nm light, [CB[7]] = 2[DTE-MPBT] = 4.0 × 10^{-5} M.

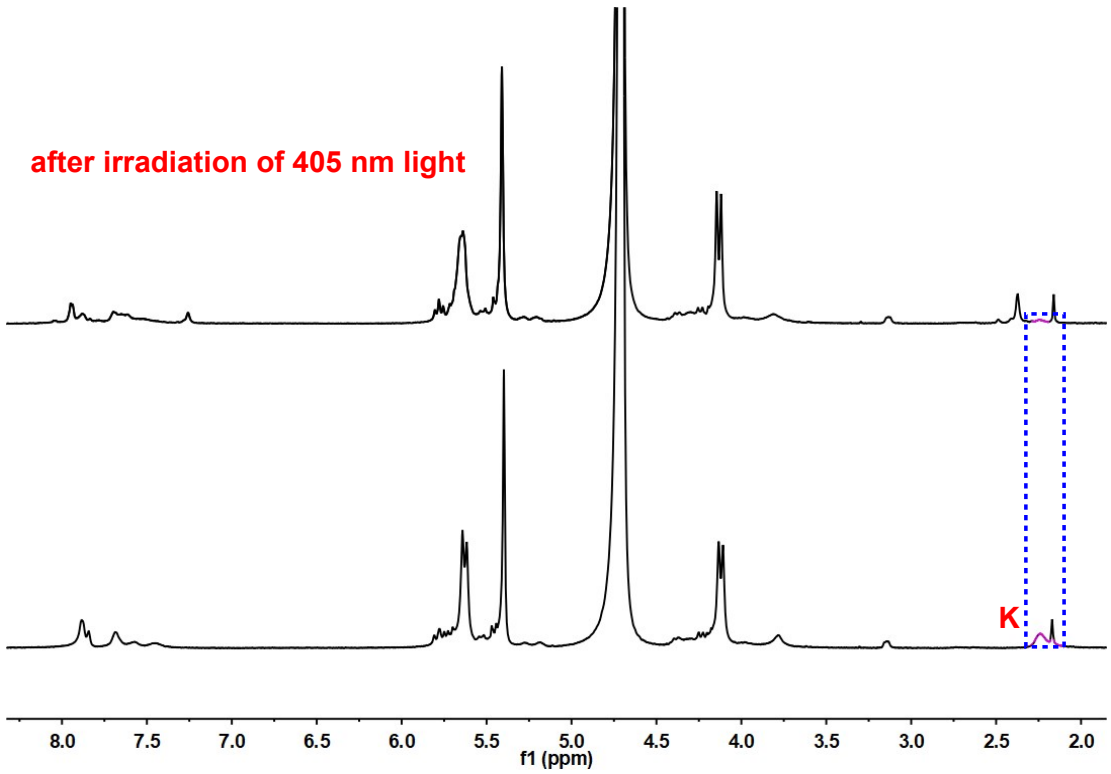

Figure S20. The variation of the ^{1}H NMR (400 MHz, D_2O) signals of DTE-MPBT⊂CB[7]$_2$ upon 405 nm light irradiation. Cyclization conversion yield is determined to be 83% through the calculation of nuclear magnetic integral area.

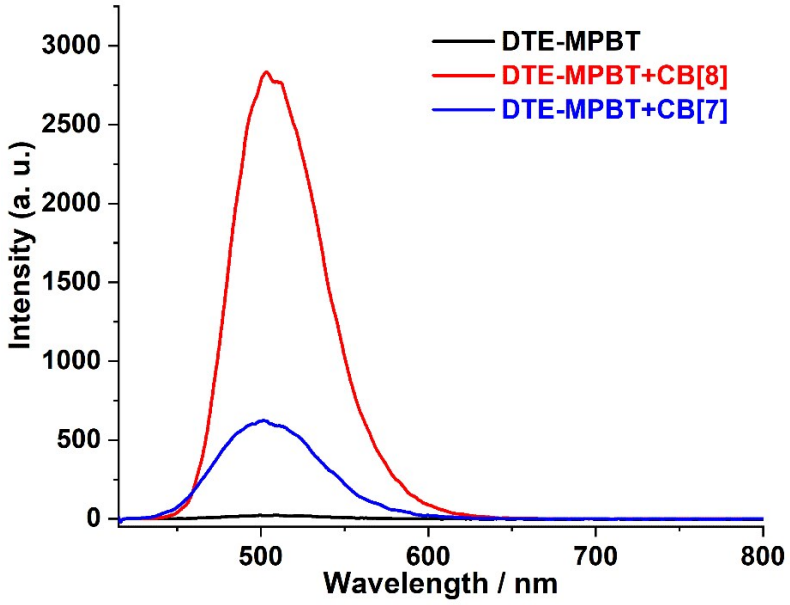

Figure S21. Fluorescence spectra of DTE-MPBT, DTE-MPBT⊂CB[7]$_2$ and DTE-

MPBT⊂CB[8], [CB[7]] = 2[CB[8]] = 2[DTE-MPBT] = 1.0 × 10^{-5} M; λ_{ex} = 405 nm; Slit = 2.5, 1.0.

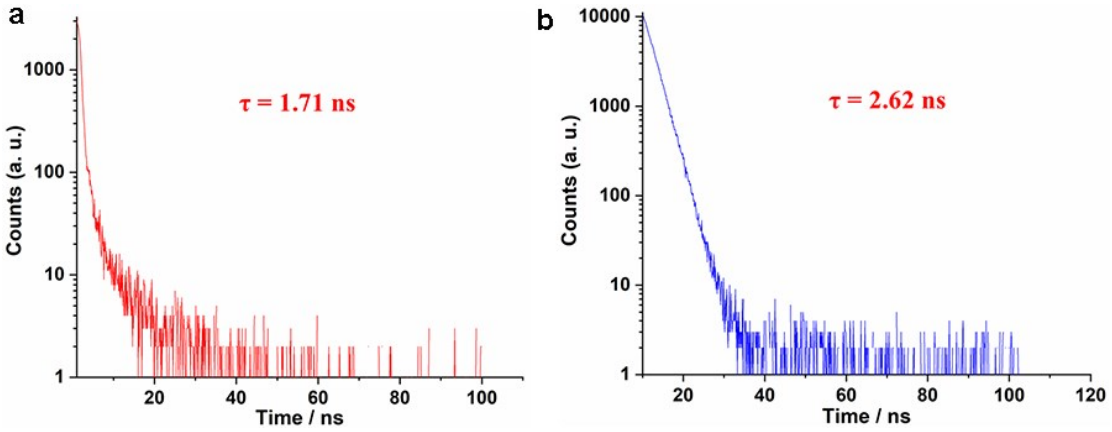

Figure S22. **a** Fluorescence decay profiles of DTE-MPBT in water; b Fluorescence decay profiles of DTE-MPBT in the presence of CB[8] in water; [DTE-MPBT] = [CB[8]] = 5 × 10^{-6} M, monitored at λ = 505 nm (λ_{ex} = 405 nm).

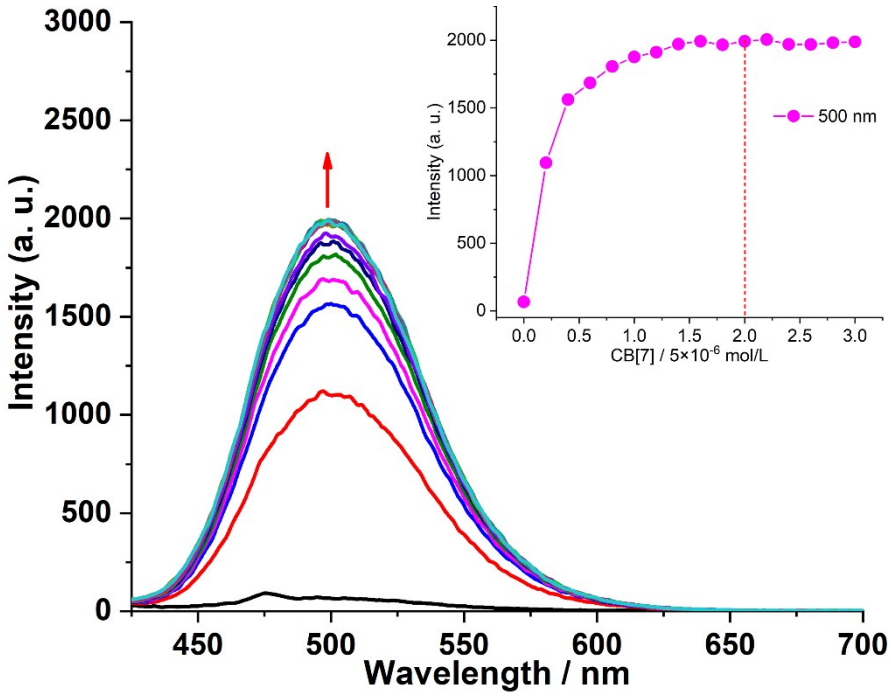

Figure S23. Fluorescence spectra of DTE-MPBT with sequential addition of 0 ～ 3 eq CB[7]; [DTE-MPBT] = 5 × 10^{-6} M; λ_{ex} = 405 nm; Slit = 5.0, 2.5.

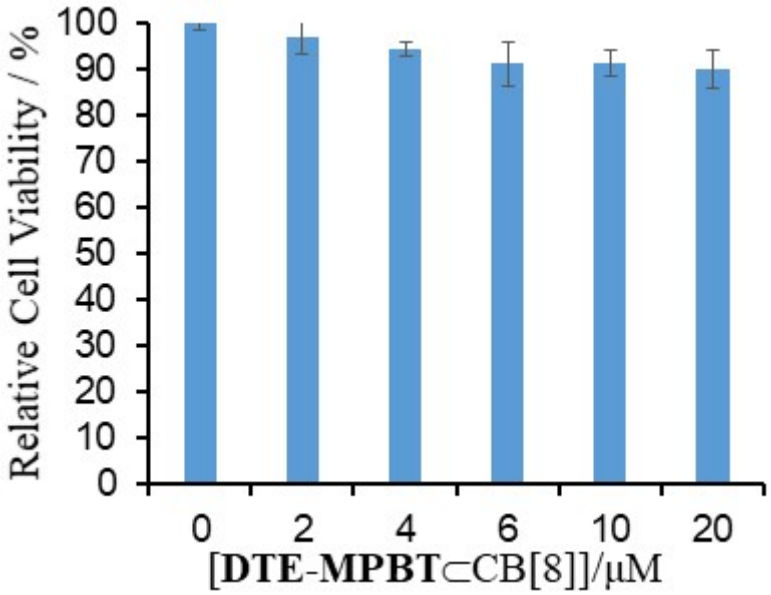

Figure S24. Relative cell viabilities of DTE-MPBT⊂CB[8] for 293T cell at different concentrations.

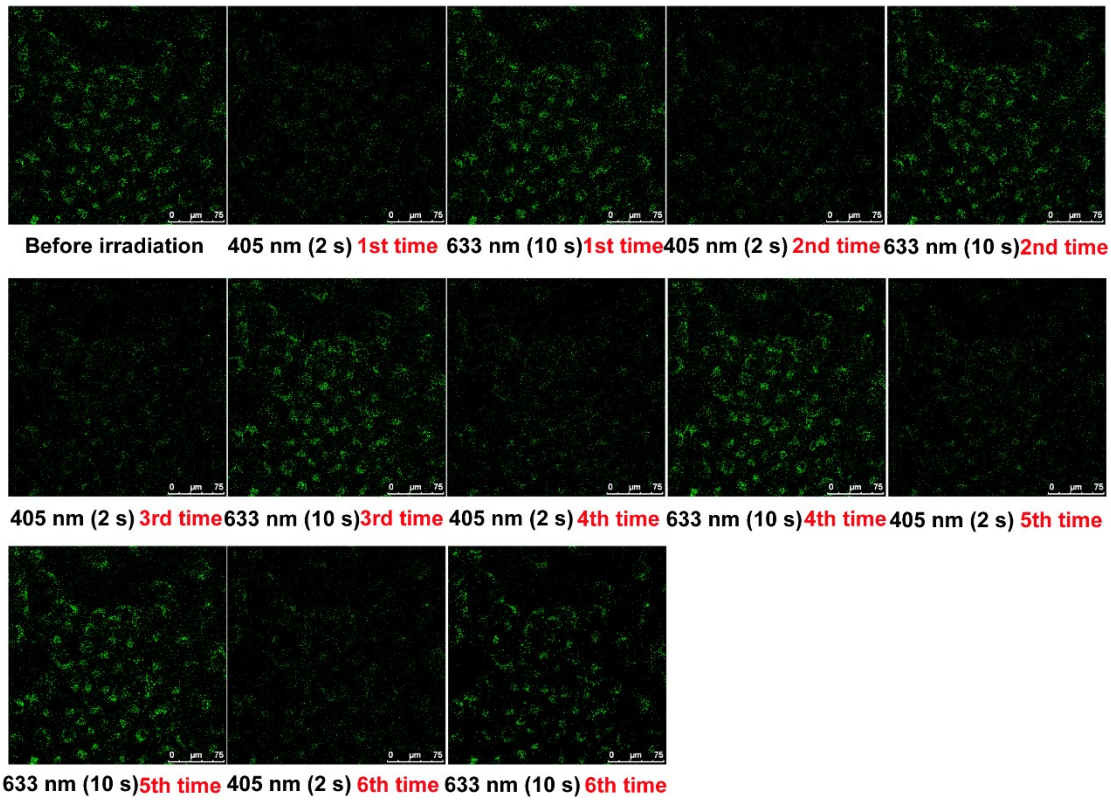

Figure S25. The variation and reciprocating test of photo-controlled confocal fluorescence images of A549 cells co-stained with [DTE-MPBT] = [CB[8]] = 1.0×10^{-5} M; The cell in the same region was irradiated by alternate 405 nm and 633 nm visible

light for six times.

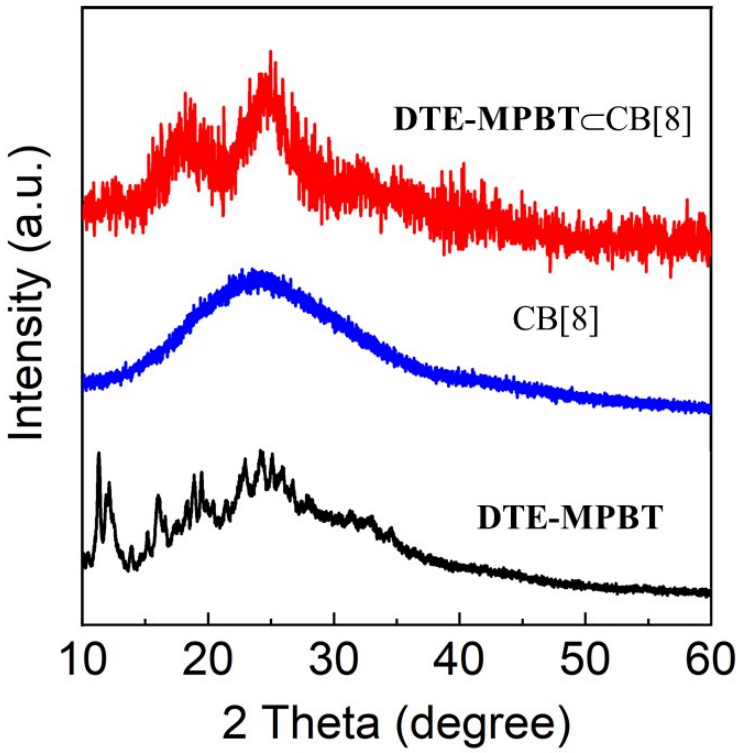

Figure S26. Powder X-ray diffraction of DTE-MPBT, CB[8] and DTE-MPBT⊂CB[8] powders.

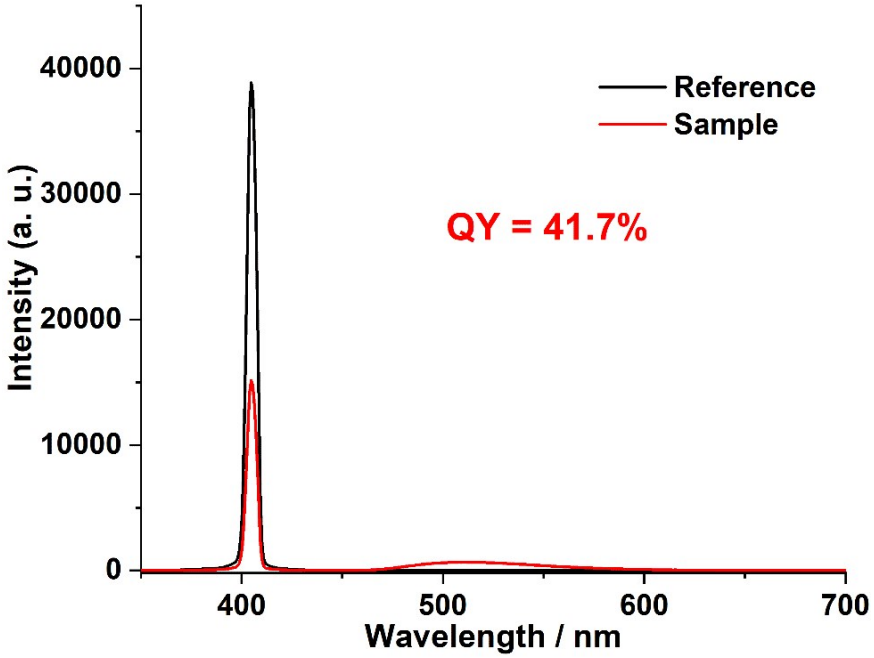

Figure S27. Absolute fluorescence quantum yield of DTE-MPBT⊂CB[8], [DTE-MPBT] = [CB[8]] = 5×10^{-6} M, λ_{ex} = 405 nm.

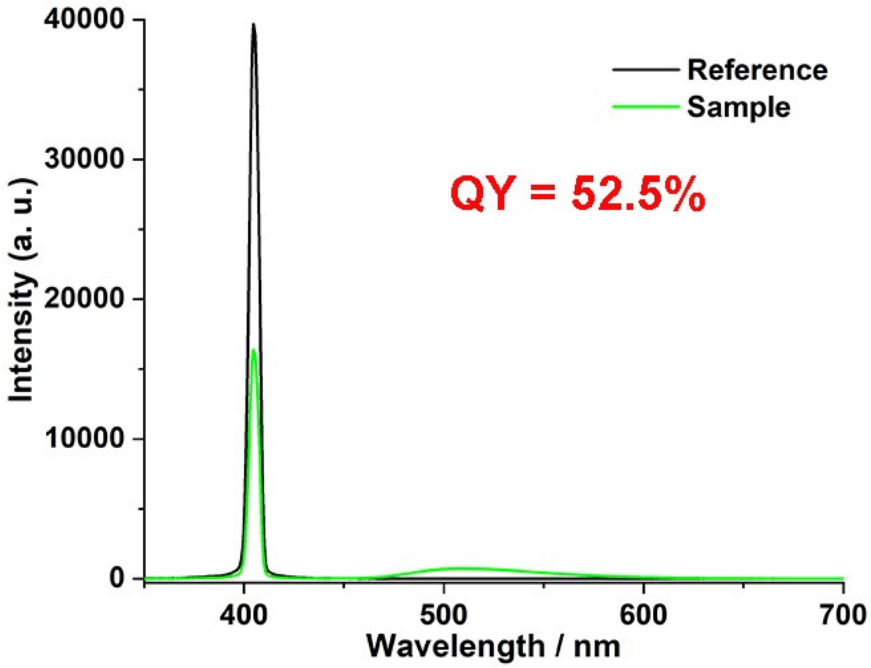

Figure S28. Absolute fluorescence quantum yield of solid-state DTE-MPBT⊂CB[8], λ_{ex} = 405 nm.

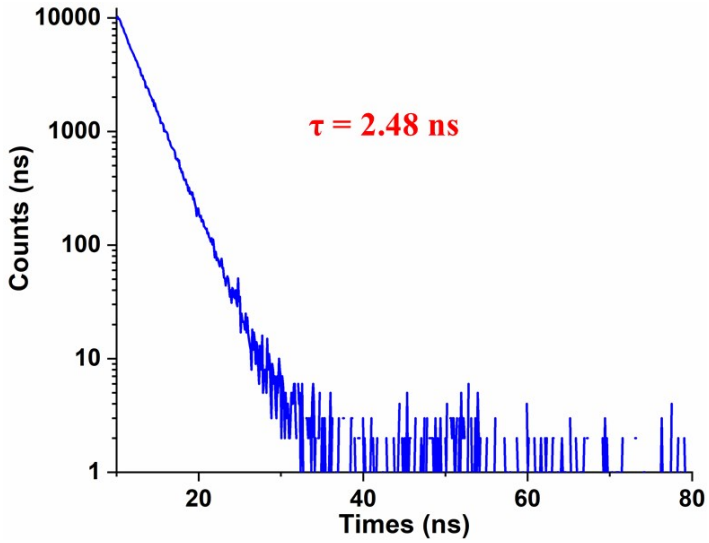

Figure S29. Fluorescence decay profiles of solid-state DTE-MPBT⊂CB[8] assembly, monitored at λ = 505 nm (λ_{ex} = 405 nm).

Relevant calculation details

Determination of complex stability constant (Ks)

Determination of Ks for DTE-MPBT and CB[8] is as follows: [1,2]

In the fluorescence spectral titration experiments, the complex stability constant (Ks) (Ks) for a stoichiometric 1:1 complex of DTE-MPBT with CB[8] was calculated by using the non-linear least-squares fit of the titration data to the following equation:

$$\Delta F = \frac{1}{2}\{\varepsilon([H]_0 + [G]_0 + \frac{1}{K_a}) \pm \sqrt{\varepsilon^2([H]_0 + [G]_0 + \frac{1}{K_a})^2 - 4\varepsilon^2[H]_0[G]_0}\}$$

where ΔF is the fluorescence intensity change of DTE-MPBT upon addition of CB[8] and defined as $\Delta F = F$ (with CB[8]) – F (without CB[8]), ε is the sensitivity factor, and $[H]_0$ and $[G]_0$ are the initial concentrations of CB[8] and guest molecules, respectively.

Determination of Ks for DTE-MPBT and CB[7] is as follows:

In the UV-vis titration experiments, the complex stability constant (Ks) for a stoichiometric 2: 1 host-guest complex (DTE-MPBT⊂CB[7]$_2$) of CB[7] with DTE-MPBT was calculated by using the non-linear least-squares fit of the titration data according to the following formula with the Origin program.[2,3]

$$\Delta A_{obs} = \frac{\varepsilon_{\Delta HG}[G]_0 K_1[H] + 2\varepsilon_{\Delta H_2G}[G]_0 K_1 K_2[H]^2}{1 + K_1[H] + K_1K_2[H]^2}$$

where ΔA_{obs} is the UV-vis absorption change of DTE-MPBT upon addition of CB[7]. K_{S1} and K_{S2} are the first-order bonding constant and the second-order bonding constant, respectively. $\varepsilon_{\Delta HG}$ is the molar absorption coefficient change between the DTE-MPBT⊂CB[7] inclusion complex and DTE-MPBT. $\varepsilon_{\Delta H_2G}$ is the molar absorption coefficient change between the DTE-MPBT⊂CB[7]$_2$ inclusion complex and DTE-MPBT. $[G]_0$ is the initial concentration of the guest molecule.

Photoreaction quantum yield measurements

The determination of photocyclization quantum yield is as follows:[4]

The light intensity at 405 nm was determined by using ferrioxalate actinometry. Therefore 3 mL of a 0.006 M solution in 0.05 M H_2SO_4 was irradiated and 0.5 mL of phenanthroline (0.1 wt% in 0.5 M H_2SO_4/1.6 M NaOAc) were added subsequently. The resulting absorbance at 510 nm was used to calculate the light intensity via formula S1

$$I_0 = \frac{\Delta A_{(510nm)}}{\Delta t \times \varepsilon_{(510nm)} \times \varphi_{irr}} \times \frac{3.5ml}{3.0ml} \qquad \text{(S1)}$$

Thereby $\Delta A_{(510nm)}$ is the difference of the absorption at 510 nm for an irradiated versus a nonirradiated solution, Δt is the irradiation time, $\varepsilon_{(510nm)}$ is 11100 M^{-1} cm^{-1} and Φ_{irr} is the quantum yield at the used irradiation wavelength (1.14 for 405 nm)

For the determination of the quantum yield formula S2 was used:

$$\varphi_x = \frac{\Delta A / \Delta t}{I_0 \times \varepsilon_x \times F_x} \qquad \text{(S2)}$$

for which $\Delta A/\Delta t$ is the change of absorbance at a wavelength, which changes upon irradiation within the time. $F_x = 1–10^{-A}$ is the percentage of the absorbed photons by the solution at irradiation wavelength, ε_x is the extinction coefficient at observed wavelength and I_0 the light intensity.

Through the above method, the photocyclization quantum yields of DTE-MPBT⊂CB[8] and DTE-MPBT⊂$CB[7]_2$ were determined to be 0.41 and 0.08, respectively.

The determination of photocycloreversion quantum yield is as follows: [5-8]

$$\varphi_{\chi} = \frac{\varepsilon_0 k_{\chi} \varphi_0}{\varepsilon_{\chi} k_0}$$

ε_0: molar absorption coefficient of the reference, εx: molar absorption coefficient of the sample; k_0: reaction rate constant of the reference, k_{χ}: reaction rate constant of the sample; φ_0: Quantum yield of the reference, φ_x: Quantum yield of the sample. The quantum yields were determined by comparing the reaction yields of diarylethenes derivatives against 1,2-bis(2-methyl-5-phenyl-3-thienyl)perfluorocyclopentene (reference substance) at room temperature ($\varphi_0 = 0.013$).

Through the above method, the photo-cycloreversion quantum yields of DTE-MPBT⊂CB[8] and DTE-MPBT⊂CB[7]$_2$ were determined to be 0.0011 and 0.0016, respectively.

Determinations of relative fluorescence quantum yield.

The relative fluorescence quantum yields were determined using the following formula: [9, 10]

$$\varphi_x = \varphi_{st}(K_x/K_{st})(\eta_x/\eta_{st})^2$$

Where φ is the QY, K is the slope determined by the curves and η is the refractive index. The subscript "*st*" refers to the standards and "*x*" refers to the unknown samples. For these aqueous solutions, $\eta_x/\eta_{st} = 1$. Coumarin 307 (ethanol as solvent; QY = 0.56) was chosen as standard. The fluorescence quantum yields are thus estimated to be 0.5% for DTE-MPBT, 46.2% for DTE-MPBT(o)⊂CB[8] and 0.6% for DTE-MPBT(c)⊂CB[8], respectively.

Computational methods.

The geometry optimization and molecule orbital calculation were carried out with B3LYP functional[11-15] and 6-31g(d) basis set, with DFT-D3(BJ) dispersion correction.[16] All calculations were carried out with Gaussian 16.[17] Computed structures were illustrated using CYLView.[18]

The structural characterization data of all new compounds

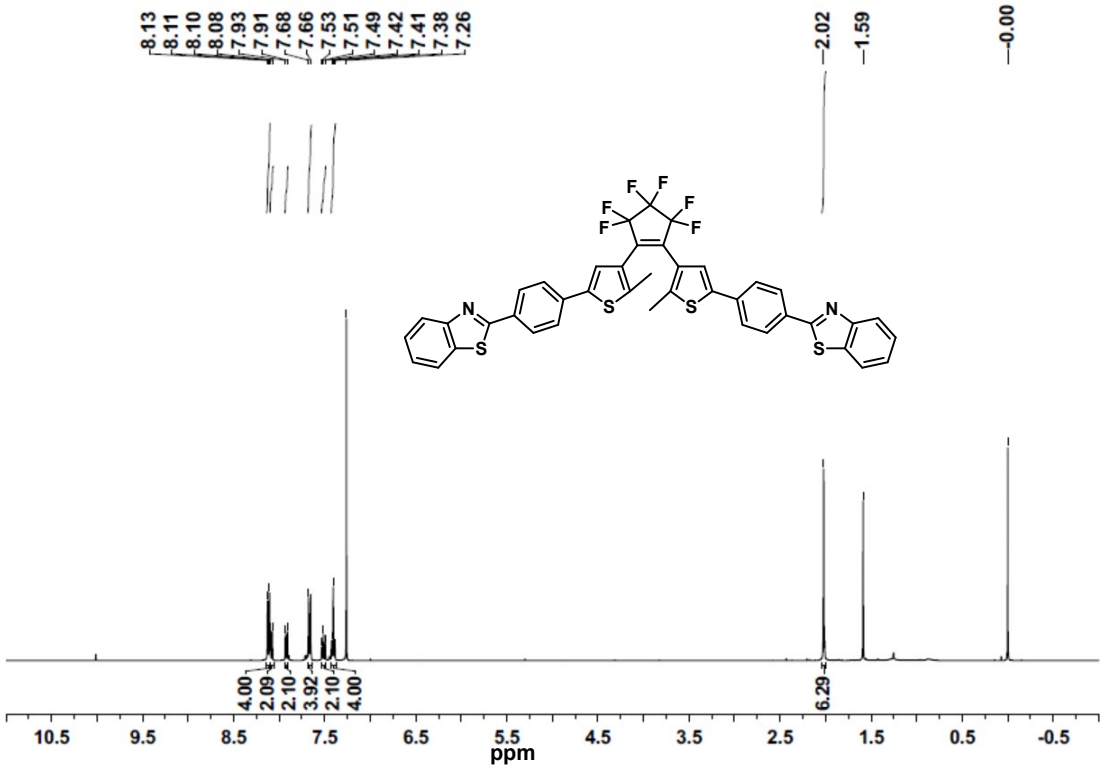

^{1}H NMR spectrum (400 MHz, $CDCl_3$) of **3**.

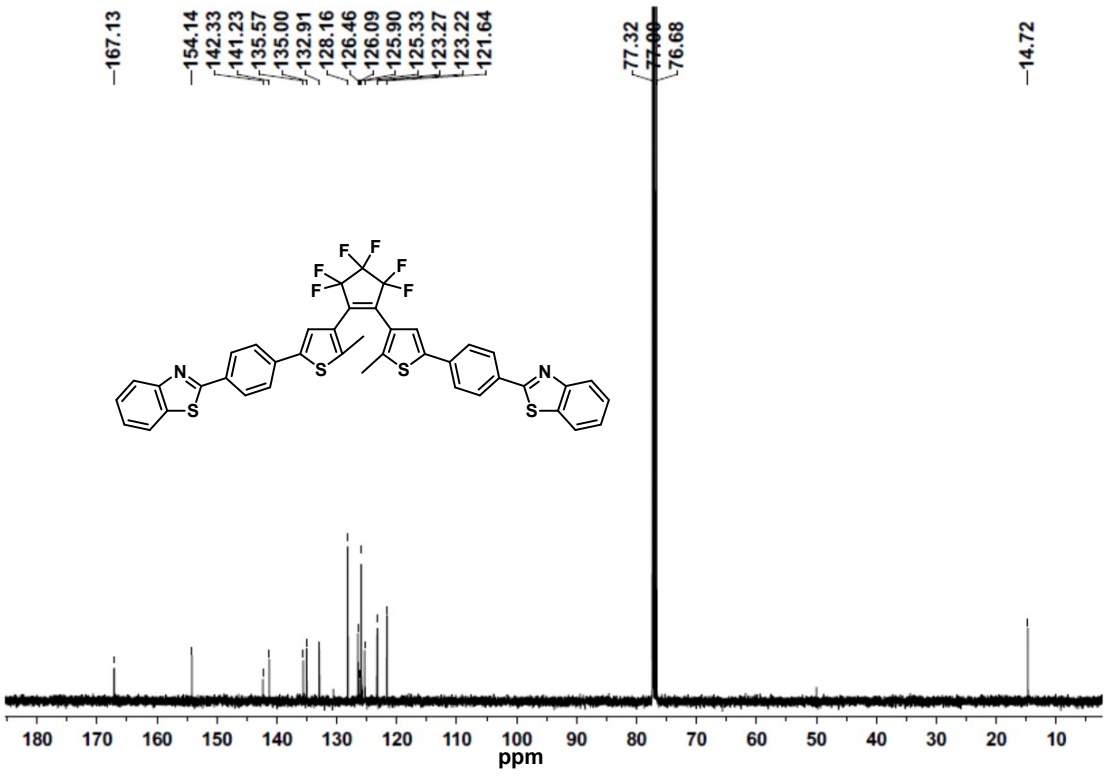

^{13}C NMR spectrum (100 MHz, $CDCl_3$) of **3**.

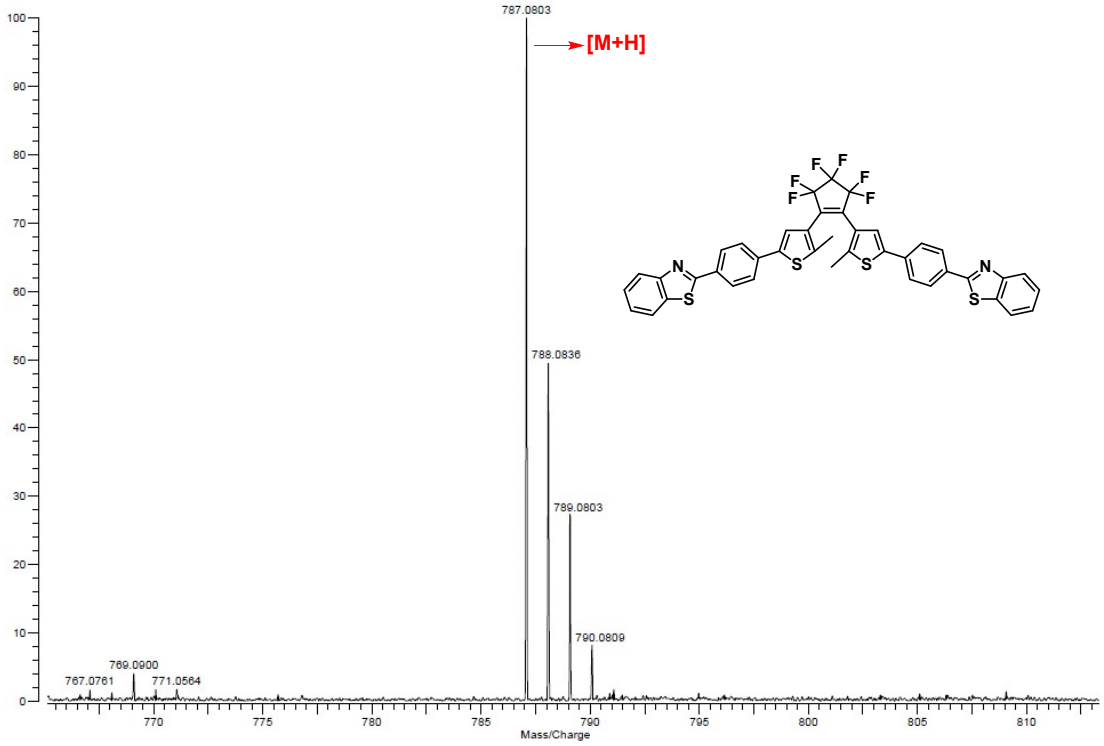

HR-MS (MALDI) of **3**.

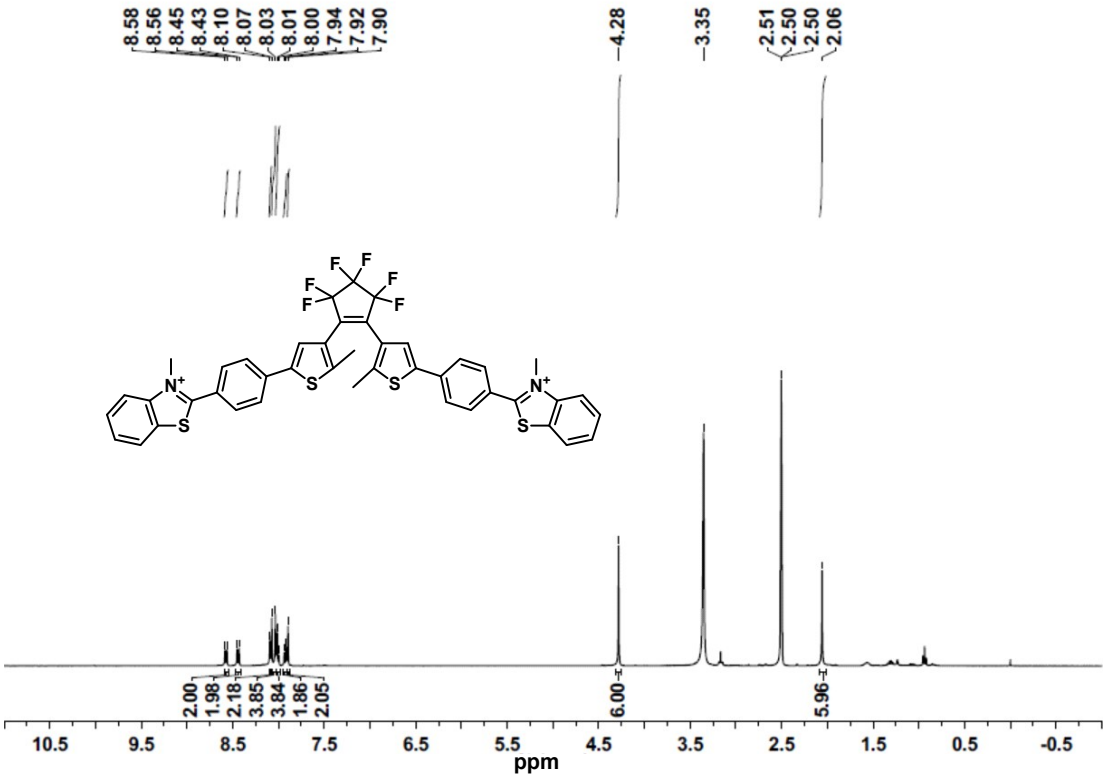

^{1}H NMR spectrum (400 MHz, DMSO) of DTE-MPBT.

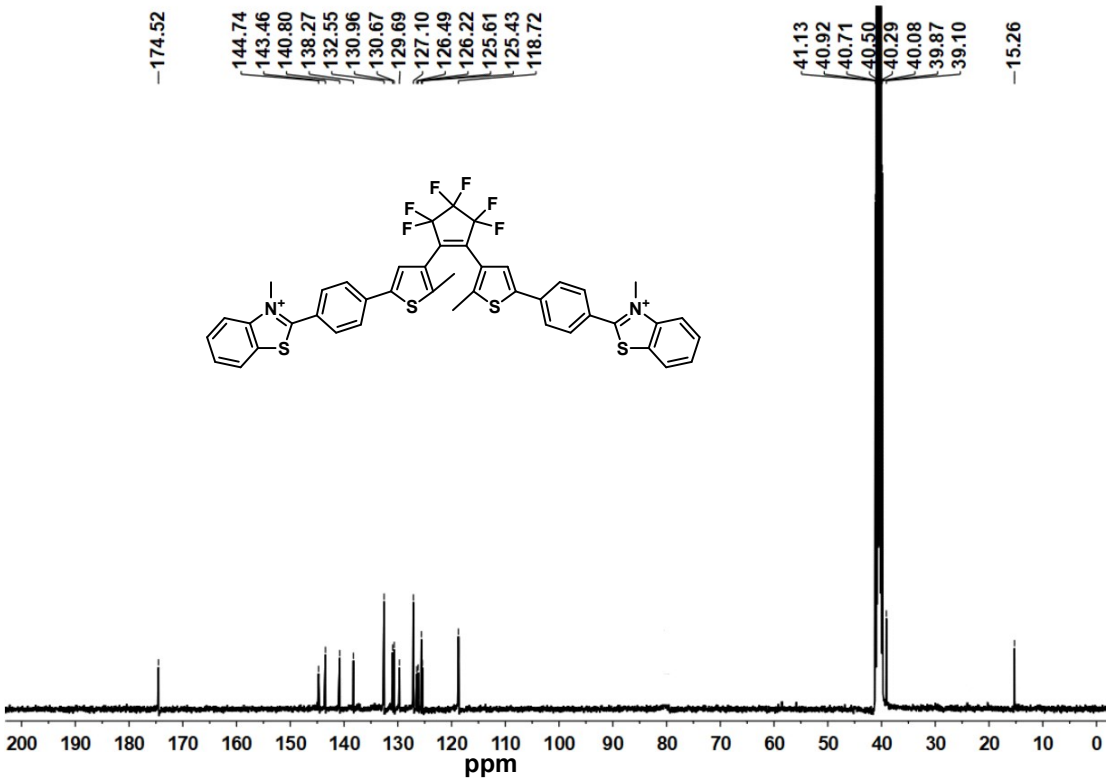

^{13}C NMR spectrum (100 MHz, DMSO) of DTE-MPBT.

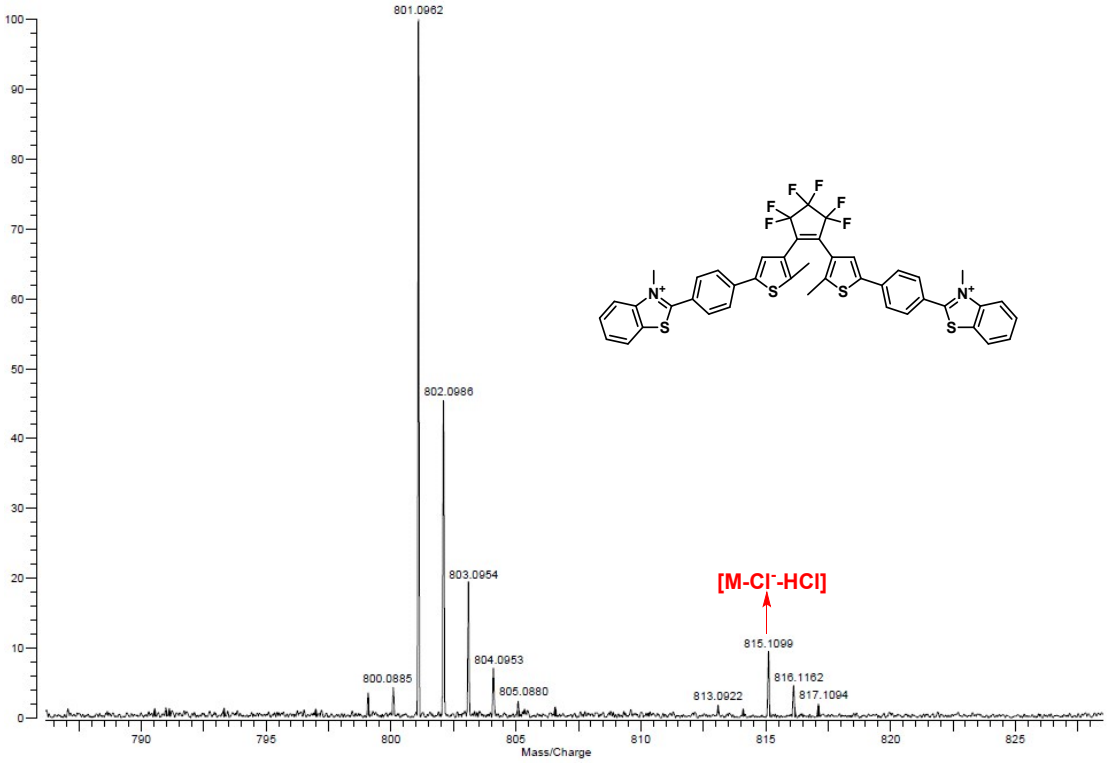

HR-MS (MALDI) of DTE-MPBT.

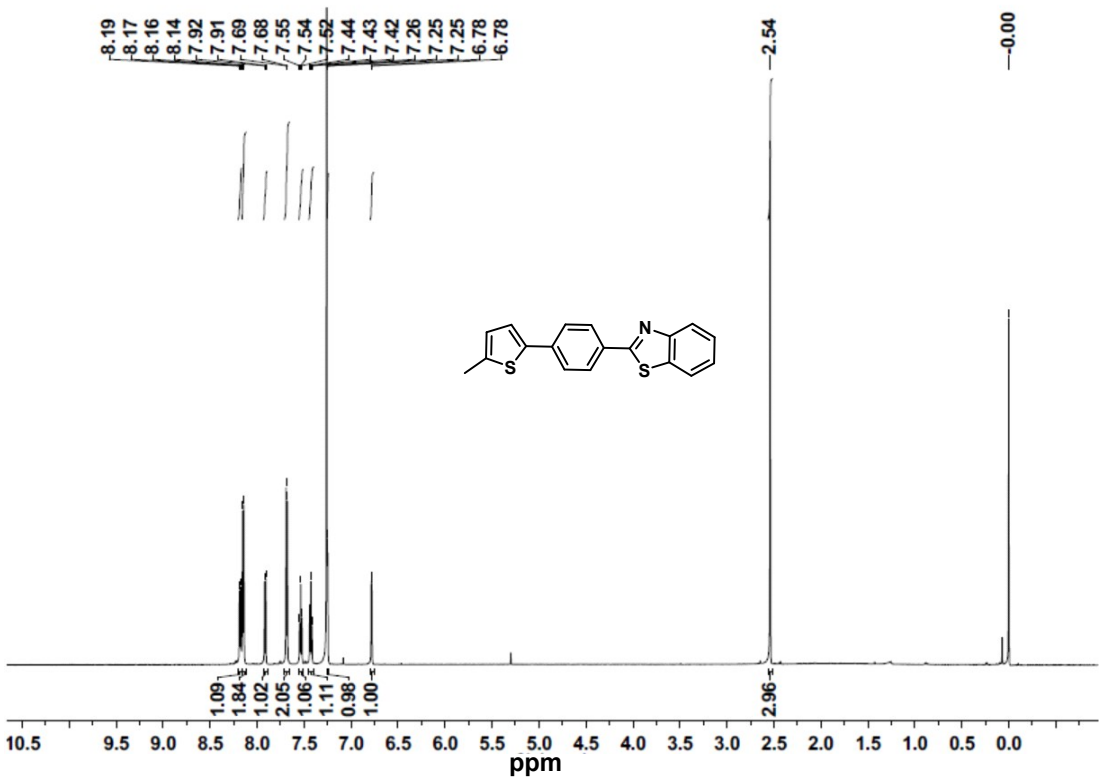

^{1}H NMR spectrum (600 MHz, $CDCl_3$) of **5**.

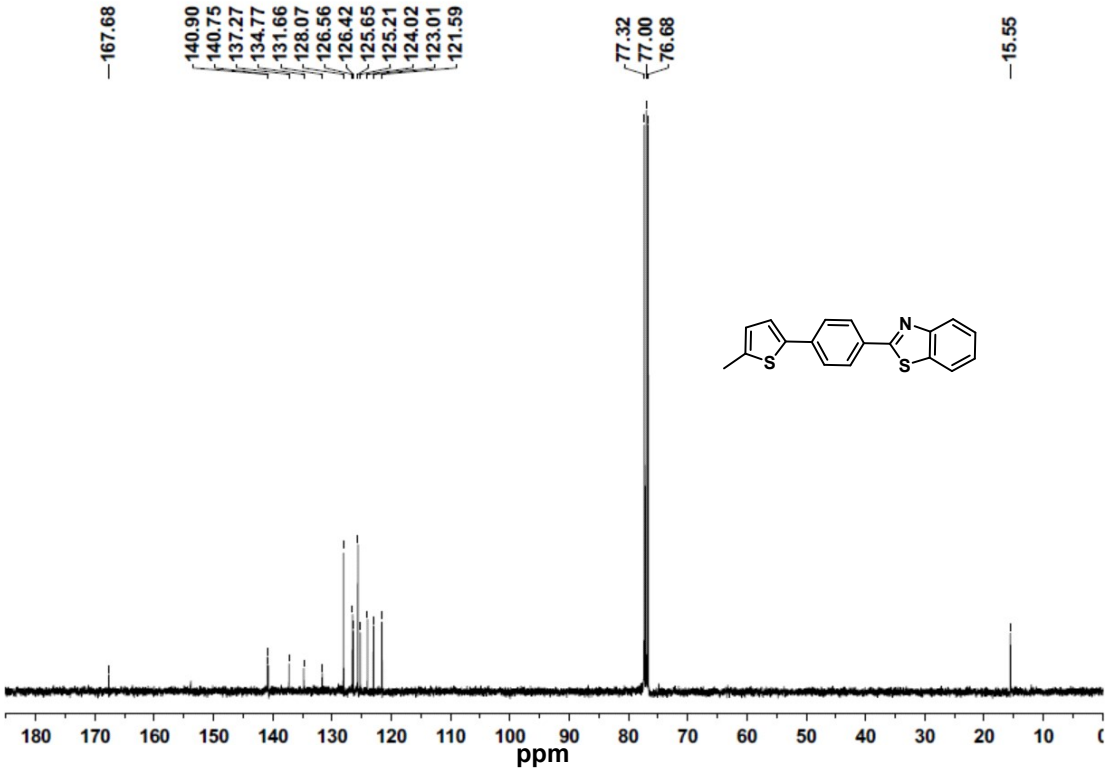

^{13}C NMR spectrum (100 MHz, $CDCl_3$) of **5**.

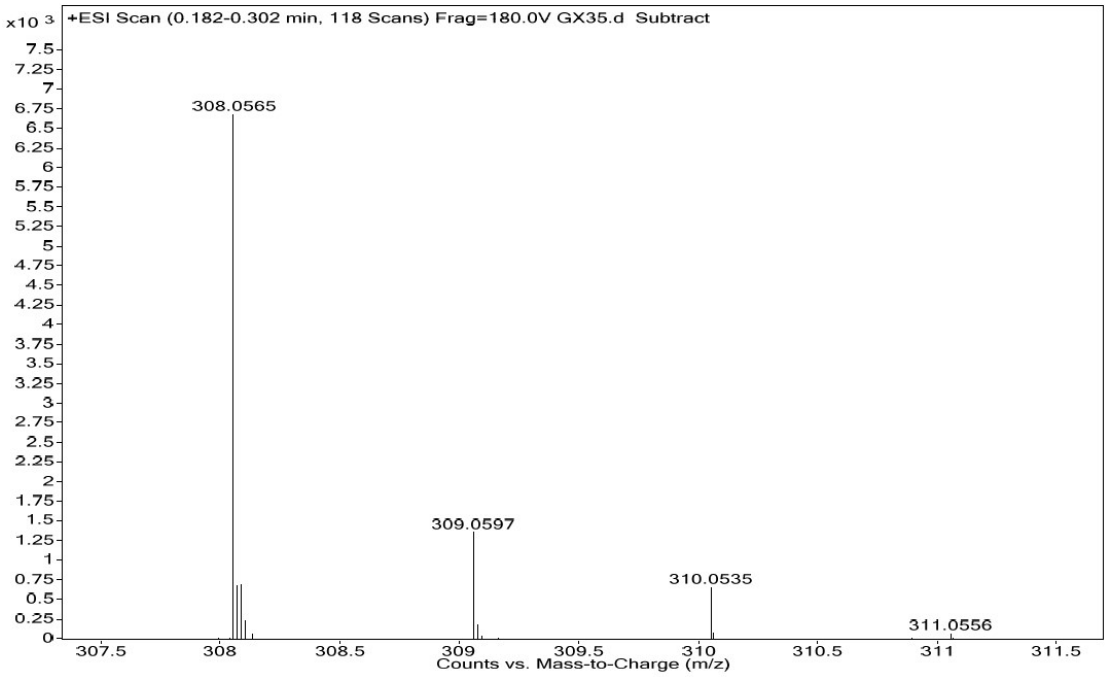

HR-MS (ESI) of **5**.

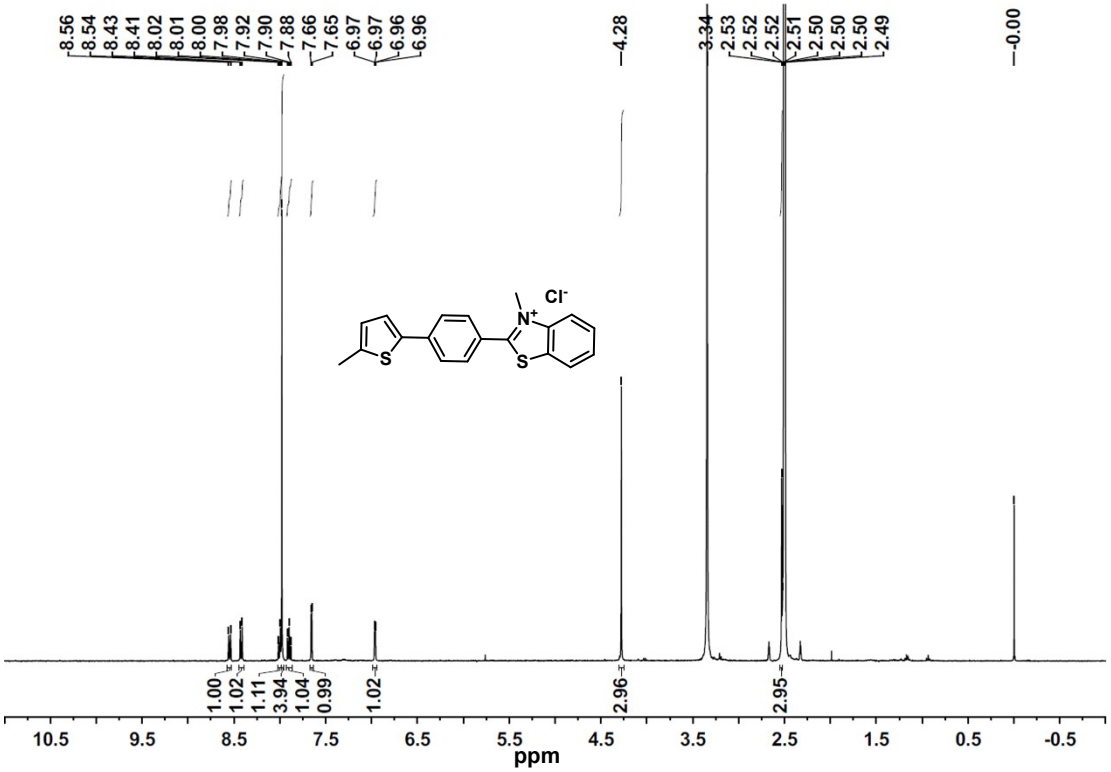

^{1}H NMR spectrum (400 MHz, DMSO) of T-MPBT.

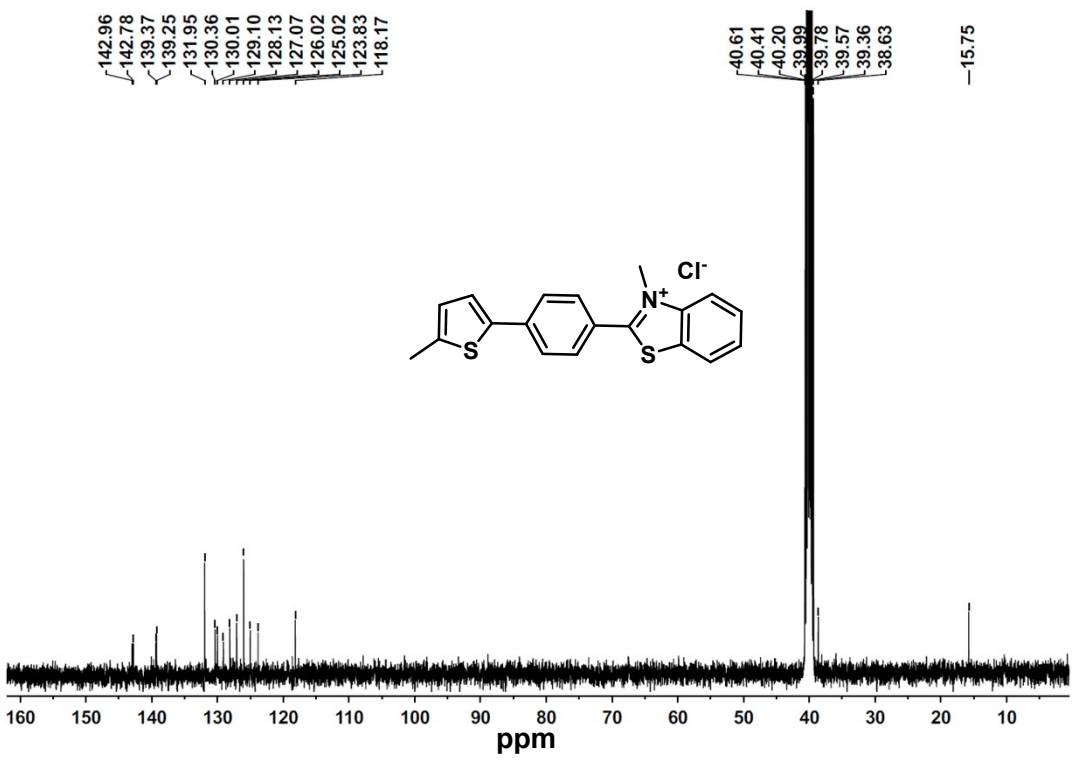

^{13}C NMR spectrum (100 MHz, DMSO) of T-MPBT.

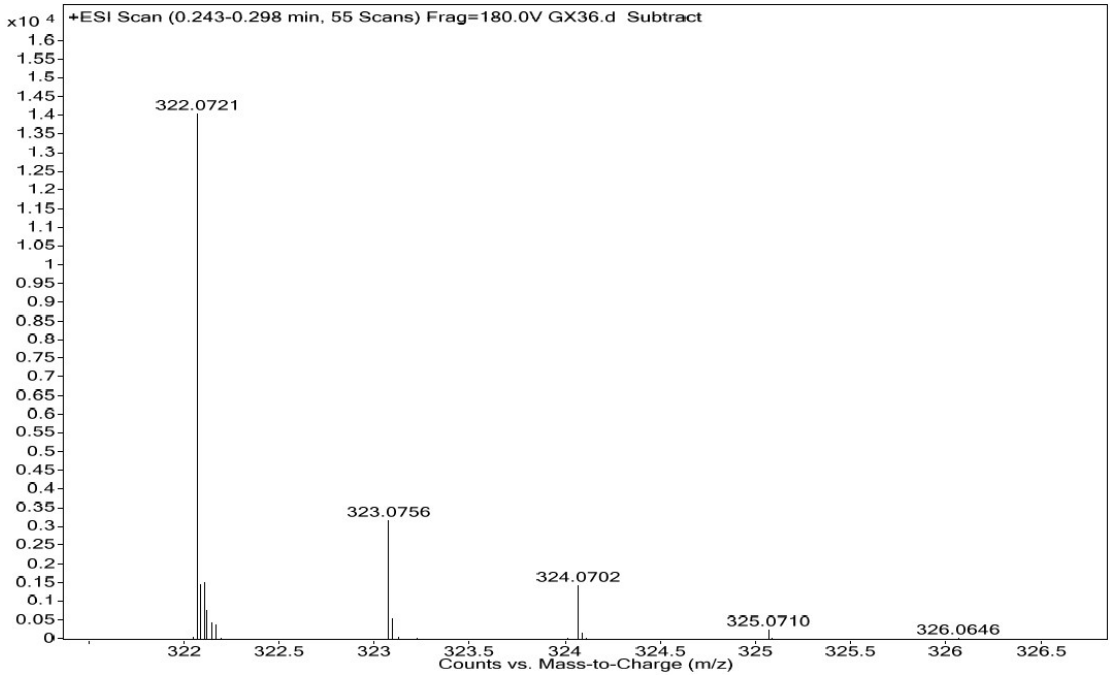

HR-MS (ESI) of T-MPBT.

The Cartesian coordinates of the species discussed in the text.

DTE-MPBT

E0 = -3957.734099 a.u.

Atom	X	Y	Z
C	2.916219	1.073756	0.218488
C	1.537226	1.125445	0.590980
H	3.373527	1.825674	-0.409338
C	1.163997	0.059379	1.397358
C	-0.154950	-0.217238	2.045885
H	-0.695990	0.718353	2.209400
H	-0.025981	-0.713987	3.011660
H	-0.784647	-0.857657	1.416597
C	-0.645177	2.183870	-0.202170
C	0.645437	2.222561	0.210437
C	-1.110351	-0.050207	-1.304617
C	-1.500014	1.055688	-0.563766
C	-2.888764	1.027979	-0.225053
S	-2.446278	-1.131201	-1.552927
H	-3.355798	1.815293	0.352341
C	0.222082	-0.362982	-1.906951
H	0.840240	-0.959814	-1.225686
H	0.764808	0.562078	-2.117844
H	0.114189	-0.920251	-2.841808
S	2.501703	-1.013511	1.666966
C	1.110240	3.652225	0.393208
C	-0.012999	4.522767	-0.224038
C	-1.235702	3.575513	-0.242548
C	-3.552383	-0.090037	-0.671346
C	3.586843	-0.024295	0.704878
F	-0.236618	5.647939	0.472621
F	0.314447	4.834573	-1.499141
F	2.303294	3.897535	-0.222395
F	1.268097	3.947777	1.709864
F	-2.009794	3.797493	0.868159
F	-2.020849	3.785454	-1.324996
C	4.988357	-0.372857	0.525756
C	5.477433	-1.660670	0.827423
C	5.907194	0.585291	0.045287
C	6.815433	-1.976582	0.666437
H	4.798882	-2.426089	1.189857
C	7.246674	0.278671	-0.113584
H	5.565713	1.584941	-0.197414
C	7.730232	-1.007828	0.206872
H	7.163989	-2.971181	0.926800
H	7.914809	1.028522	-0.523145
C	-4.959221	-0.425364	-0.508665
C	-5.448286	-1.722251	-0.767935
C	-5.882674	0.555181	-0.085910
C	-6.790723	-2.026087	-0.620747
H	-4.766581	-2.504527	-1.085688
C	-7.226446	0.260618	0.058670
H	-5.541042	1.562011	0.124653
H	-7.138786	-3.029083	-0.847345
H	-7.898731	1.028960	0.424837
C	-7.709621	-1.035997	-0.218598
C	-9.105239	-1.386754	-0.030362
S	-9.559698	-2.883299	0.712981
C	-11.410089	-1.214400	-0.019874
C	-11.260619	-2.482740	0.564171
N	-10.171959	-0.642372	-0.358163
C	-12.368299	-3.235026	0.955698
C	-13.628516	-2.682548	0.751782
C	-13.779227	-1.411124	0.172516
C	-12.677421	-0.660292	-0.221115
H	-12.250643	-4.214668	1.405670
H	-14.508826	-3.242719	1.048251
H	-14.774409	-1.003796	0.030753
H	-12.804775	0.322661	-0.659383
C	-10.113858	0.607977	-1.130481
H	-10.307871	1.462605	-0.477754
H	-9.132143	0.702580	-1.588536
H	-10.874857	0.561183	-1.910905
C	9.120827	-1.372020	0.007902
S	9.556498	-2.899654	-0.681607
C	11.425816	-1.210559	-0.050031
C	11.261300	-2.500980	-0.579049
N	10.196024	-0.619687	0.286307
C	12.359065	-3.273627	-0.958640
C	13.624781	-2.719016	-0.799398
C	13.790468	-1.425695	-0.275368
C	12.698589	-0.654437	0.106274
H	12.229801	-4.270312	-1.365983
H	14.497610	-3.294848	-1.087877
H	14.789526	-1.017422	-0.167665
H	12.837386	0.345010	0.501658
C	10.156281	0.661035	1.008370
H	10.341039	1.487881	0.318247
H	9.183478	0.777938	1.480090
H	10.931332	0.642715	1.776043

DTE-MPBT⊂CB[8]

E0 = -3957.720177 a.u.

Atom	X	Y	Z
C	-2.849116	0.770412	-0.040383
C	-1.474961	0.834119	-0.425968
H	-3.367946	1.593613	0.428286
C	-1.051512	-0.304703	-1.098735
C	0.283146	-0.614581	-1.699738
H	0.810140	0.303249	-1.972653
H	0.180893	-1.229976	-2.598230
H	0.934493	-1.157393	-1.006578
C	0.643846	2.085076	0.230032
C	-0.643993	2.015187	-0.187684
C	1.181856	0.047103	1.625398
C	1.527816	1.016628	0.696169
C	2.870962	0.879948	0.232106
S	2.499432	-1.046758	1.904239
H	3.321512	1.557128	-0.479718
C	-0.121993	-0.144655	2.334680
H	-0.785026	-0.819095	1.778301
H	-0.645352	0.810773	2.430214
H	0.024782	-0.559944	3.336406
S	-2.349363	-1.454392	-1.234556
C	-1.176878	3.389240	-0.532315
C	-0.108245	4.375249	-0.001525
C	1.158638	3.500615	0.149374
C	3.532265	-0.195009	0.775265
C	-3.471346	-0.405930	-0.386046
F	0.082043	5.426234	-0.821607
F	-0.481361	4.826673	1.219903
F	-2.389096	3.655961	0.027374
F	-1.315721	3.534281	-1.880132
F	1.968321	3.678999	-0.939085
F	1.870585	3.867834	1.249767
C	-4.877614	-0.717254	-0.216047
C	-5.521274	-1.729977	-0.953994
C	-5.664429	0.071644	0.643630
C	-6.887279	-1.905674	-0.867350
H	-4.963103	-2.355795	-1.639500
C	-7.036044	-0.077893	0.702260
H	-5.210661	0.841718	1.249907
C	-7.694197	-1.081901	-0.045872
H	-7.343109	-2.677594	-1.476734
H	-7.585126	0.630664	1.301843
C	4.913073	-0.572501	0.529073
C	5.706415	-1.186489	1.517001
C	5.506927	-0.307482	-0.720222
C	7.047240	-1.423139	1.290548
H	5.279132	-1.449850	2.477957
C	6.845699	-0.576094	-0.959959
H	4.884706	0.086557	-1.512292
H	7.624394	-1.869747	2.091063
H	7.225263	-0.413485	-1.958763
C	7.674819	-1.084903	0.066813
C	9.111608	-1.281208	-0.035479
S	9.940916	-2.226667	1.163558
C	11.302079	-1.158179	-0.754739
C	11.477814	-1.935643	0.398652
N	9.963913	-0.779678	-0.942124
C	12.740916	-2.350603	0.817101
C	13.828307	-1.978510	0.033945
C	13.655389	-1.223221	-1.138880
C	12.395916	-0.802682	-1.549588
H	12.852251	-2.940013	1.717959
H	14.826248	-2.284983	0.329505
H	14.520357	-0.964233	-1.740305
H	12.272631	-0.233775	-2.462924
C	9.636156	0.199967	-1.987793
H	9.420443	-0.317342	-2.920035
H	8.798230	0.808604	-1.661100
H	10.488319	0.858959	-2.127492
C	-9.128937	-1.266152	-0.070148
S	-9.878396	-2.222225	-1.315216
C	-11.378817	-1.059360	0.449160
C	-11.468173	-1.909837	-0.660944
N	-10.044208	-0.763553	0.778037
C	-12.693805	-2.374555	-1.131588
C	-13.833893	-1.954920	-0.454647
C	-13.749655	-1.078639	0.641758
C	-12.526967	-0.612674	1.109056
H	-12.739098	-3.022687	-1.997717
H	-14.807378	-2.293317	-0.794123
H	-14.659660	-0.743953	1.128388
H	-12.474992	0.097422	1.925999
C	-9.736538	-0.095637	2.047073
H	-8.839092	-0.535178	2.479490
H	-9.594960	0.971702	1.884977
H	-10.571879	-0.249656	2.725388

DTE-MPBT⊂CB[8]

E0 = -15573.952270 a.u.

Atom	X	Y	Z
C	-2.371094	-2.386126	0.276496
C	-1.034150	-2.307200	0.773878
H	-2.691685	-3.133244	-0.434509
C	-0.880070	-1.331880	1.750531
C	0.333051	-0.962986	2.544756
H	1.014836	-1.812785	2.632091
H	0.063306	-0.636243	3.553186
H	0.901314	-0.149796	2.080892
C	1.321687	-2.946085	0.048323
C	0.024631	-3.217299	0.334661
C	1.522692	-0.549071	-0.728693
C	2.001970	-1.654012	-0.041285
C	3.264883	-1.411434	0.578621
S	2.612336	0.793623	-0.586783
H	3.800764	-2.163125	1.140808
C	0.246861	-0.408285	-1.498309
H	-0.565002	-0.033360	-0.862423
H	-0.072300	-1.380633	-1.883732
H	0.362934	0.277215	-2.343341
S	-2.384198	-0.506439	2.034951
C	-0.245250	-4.705034	0.267089
C	1.023609	-5.310749	-0.380239
C	2.099859	-4.218757	-0.175332
C	3.730065	-0.131903	0.393465
C	-3.230400	-1.472306	0.839488
F	1.372419	-6.491304	0.165595
F	0.813166	-5.479918	-1.707635
F	-1.349233	-5.022455	-0.463890
F	-0.425438	-5.224879	1.513772
F	2.868808	-4.534486	0.911491
F	2.928535	-4.149388	-1.252861
C	-4.659157	-1.379414	0.608325
C	-5.528435	-0.728639	1.505721
C	-5.227722	-2.037316	-0.498193
C	-6.895588	-0.779363	1.324987
H	-5.142200	-0.219286	2.380080
C	-6.596733	-2.121265	-0.659093
H	-4.599205	-2.526452	-1.227716
C	-7.479034	-1.484004	0.244424
H	-7.526655	-0.289665	2.057750
H	-6.962429	-2.730266	-1.470528
C	4.994227	0.403428	0.867868
C	5.703412	1.387344	0.152787
C	5.560249	-0.075100	2.065476
C	6.957215	1.787378	0.568776
H	5.285205	1.817026	-0.750452
C	6.805035	0.351342	2.502045
H	4.985879	-0.768410	2.664827
H	7.477578	2.524834	-0.030199
H	7.154656	-0.001281	3.462014
C	7.572043	1.252167	1.726930
C	8.934437	1.663811	2.023228
S	9.625004	3.024321	1.191685
C	11.064167	1.741481	2.911402
C	11.145510	2.815662	2.014094
N	9.818526	1.097550	2.858510
C	12.322973	3.542312	1.845934
C	13.418400	3.172892	2.619094
C	13.334401	2.115065	3.540955
C	12.162006	1.385821	3.700641
H	12.364638	4.359842	1.137942
H	14.350993	3.717429	2.514615
H	14.199644	1.861996	4.144500
H	12.103934	0.582310	4.424543
C	9.633968	-0.166413	3.585756
H	9.270630	0.038432	4.590366
H	8.951101	-0.803978	3.032140
H	10.590337	-0.678283	3.643338
C	-8.921151	-1.568167	0.165490
S	-9.910248	-1.124376	1.525893
C	-11.054934	-2.022029	-0.618974
C	-11.369748	-1.526379	0.653366
N	-9.672432	-1.980331	-0.871545
C	-12.686466	-1.426443	1.095983
C	-13.683410	-1.844987	0.221302
C	-13.369268	-2.369635	-1.044845
C	-12.055368	-2.472158	-1.484858
H	-12.905144	-1.050056	2.087355
H	-14.721342	-1.785606	0.532108
H	-14.167970	-2.717723	-1.691253
H	-11.820611	-2.919169	-2.443714
C	-9.171240	-2.222321	-2.228554
H	-8.355820	-1.532980	-2.441836
H	-8.831351	-3.252206	-2.325219
H	-9.982668	-2.043122	-2.929339

C	6.307006	4.691493	-1.952292
C	7.260265	6.354142	-0.578554
C	8.011077	6.309012	-1.947017
C	9.534457	5.899442	-0.199963
C	7.341205	5.206864	-4.146717
C	10.472639	5.887273	-2.477735
C	8.146893	3.238192	-5.371242
C	9.802295	4.774321	-4.675528
C	10.476383	3.596113	-5.452667
C	11.395503	3.738094	-3.282225
C	9.436372	1.620292	-6.717576
C	12.425018	2.089577	-4.801967
C	9.114668	-0.555326	-5.577035
C	11.341775	0.096847	-5.957044
C	11.314256	-1.413731	-5.561742
C	12.712970	-0.247059	-4.068563
C	9.334090	-2.948990	-5.123708
C	12.730834	-2.711924	-3.866798
C	8.389667	-4.120141	-3.188952
C	10.727969	-4.227875	-3.431096
C	10.307226	-4.986867	-2.135910
C	11.952071	-3.385659	-1.611119
C	8.181232	6.442689	1.803222
C	5.107678	5.213873	0.117103
N	6.326094	5.239530	-0.670087
N	7.242315	5.364865	-2.714285
N	8.316506	6.189464	0.386995
N	9.341469	5.865373	-1.572359
N	8.415876	4.354762	-4.589696
N	9.351430	2.805748	-5.894494
N	10.513966	4.799812	-3.422814
N	11.329730	2.979582	-4.448469
N	9.949301	0.445300	-6.055676
N	9.918953	-1.627532	-5.203172
N	12.053629	0.700596	-4.847411
N	12.267402	-1.491736	-4.483769
N	9.492194	-3.581652	-3.838181
N	8.869859	-4.932912	-2.172978
N	11.779834	-3.355233	-2.986779
N	10.952480	-4.215515	-1.081240
O	5.577968	3.792030	-2.337068
O	7.050659	2.746548	-5.562287
O	7.901635	-0.508045	-5.520291
O	7.221149	-3.936378	-3.469648
O	10.589352	5.718513	0.383637
O	12.109695	3.525606	-2.320891
O	12.828484	-2.831410	-0.982903
C	10.119305	-4.266066	2.402133
C	8.937616	-5.727828	0.980183
C	8.197504	-5.619283	2.346866
C	6.778278	-4.885082	0.611285
C	9.008333	-4.700956	4.580036
C	5.801333	-4.963697	2.868539
C	8.314362	-2.584128	5.638127
C	6.580933	-4.094525	5.136912
C	6.016881	-2.939873	6.029332
C	4.765086	-3.071660	4.042958
C	7.173039	-0.890051	7.011399
C	3.907338	-1.506016	5.751470
C	7.301503	1.397720	6.091275
C	5.138036	0.583018	6.555922
C	5.043398	2.073627	6.081072
C	3.711607	0.716355	4.678543
C	6.900139	3.779551	5.640353
C	3.617762	3.141217	4.250488
C	7.839921	4.773949	3.597656
C	5.491272	4.817488	3.810917
C	5.909395	5.541264	2.493519
C	4.363013	3.833194	1.995766
C	7.988826	-5.750065	-1.381685
C	11.165482	-4.778056	0.234349
N	10.000105	-4.738948	1.096947
N	9.099076	-4.836337	3.147270
N	7.915878	-5.406152	0.020711
N	6.951355	-4.958033	1.991335
N	7.988082	-3.795717	5.055379
N	7.135065	-2.018235	6.108465
N	5.828827	-3.948683	3.899918
N	4.868980	-2.480154	5.289386
N	6.553924	0.302749	6.488031
N	6.422384	2.434849	5.842981
N	4.310416	-0.125804	5.606067
N	4.198077	1.994599	4.908829
N	6.743401	4.272325	4.291082
N	7.349929	5.500345	2.516235
N	4.508999	3.858844	3.372053
N	5.281568	4.734345	1.463925
O	10.975955	-3.509890	2.823142

O	9.430339	-2.112036	5.742678
O	8.515717	1.449998	6.004025
O	9.007792	4.625277	3.895713
O	5.793006	-4.460641	0.033845
O	3.876756	-2.871457	3.233113
O	2.888724	0.397621	3.842168
O	3.553801	3.177963	1.367860
H	6.717569	7.292891	-0.405985
H	8.055455	7.277094	-2.462666
H	6.415486	4.747039	-4.496680
H	7.450226	6.206431	-4.588658
H	11.368910	5.823751	-1.858710
H	10.474914	6.832829	-3.036990
H	9.883478	5.743167	-5.185341
H	11.076074	3.922757	-6.311394
H	8.418944	1.400038	-7.044370
H	10.069844	1.834000	-7.585906
H	13.198366	2.185730	-4.037643
H	12.828938	2.406141	-5.774525
H	11.855865	0.295282	-6.906838
H	11.603165	-2.087005	-6.379551
H	8.261261	-2.847149	-5.298382
H	9.779084	-3.582958	-5.906661
H	13.603387	-2.450437	-3.265588
H	13.017474	-3.421647	-4.652705
H	11.092905	-4.890389	-4.228592
H	10.651776	-6.030507	-2.110226
H	9.182151	6.387300	2.234360
H	7.773239	7.453894	1.942159
H	4.405046	4.540057	-0.374626
H	4.684191	6.232078	0.138314
H	9.356856	-6.722896	0.781895
H	7.998094	-6.588262	2.823079
H	9.965075	-4.311125	4.931015
H	8.829803	-5.693896	5.011363
H	4.916499	-4.782009	2.256488
H	5.721674	-5.954050	3.343262
H	6.424969	-5.094950	5.562214
H	5.718449	-3.266218	7.034321
H	8.224279	-0.660784	7.195879
H	6.681926	-1.160300	7.956050
H	3.005493	-1.637820	5.151686
H	3.688433	-1.707331	6.807281
H	4.768007	0.422819	7.577327
H	4.598814	2.745355	6.827735
H	7.969265	3.783661	5.860407
H	6.374487	4.449447	6.336315
H	2.793118	2.770012	3.639235
H	3.238248	3.838869	5.010061
H	5.054521	5.489520	4.563183
H	5.557499	6.581294	2.435451
H	6.987788	-5.633457	-1.799937
H	8.304027	-6.799415	-1.458844
H	11.952518	-4.193213	0.711799
H	11.498667	-5.824835	0.138522
C	-6.738982	4.309979	-3.762190
C	-8.728288	4.225332	-5.010686
C	-8.833153	5.367071	-3.958832
C	-10.668291	3.924496	-3.713906
C	-7.198434	6.107607	-2.165723
C	-10.822387	6.113136	-2.551170
C	-7.285803	5.893747	0.269650
C	-9.167420	6.884141	-0.755572
C	-9.319855	6.958885	0.799473
C	-11.187396	5.846718	-0.120620
C	-7.625990	6.454518	2.649242
C	-11.148982	6.075682	2.335337
C	-7.277747	4.429120	4.012461
C	-9.435977	5.388813	4.116084
C	-9.381520	4.121002	5.033394
C	-11.089982	3.858955	3.427308
C	-7.376835	2.713525	5.782224
C	-10.916409	2.093483	5.118990
C	-6.880098	0.440384	4.913208
C	-8.957044	0.720496	5.971147
C	-8.657430	-0.802470	5.837955
C	-10.647493	-0.311991	4.696235
C	-10.247310	2.244190	-5.439502
C	-6.659955	2.991767	-5.850030
N	-7.366625	3.785940	-4.882366
N	-7.658379	5.139328	-3.130529
N	-9.751734	3.285232	-4.565272
N	-10.101850	5.131341	-3.330122
N	-7.950036	6.108320	-0.931597
N	-8.073538	6.419406	1.280860
N	-10.387939	6.245471	-1.179941
N	-10.492766	6.146645	1.051130
N	-8.130471	5.382416	3.479512

N	-8.006053	3.693576	4.931919
N	-10.558990	5.124821	3.251948
N	-10.349442	3.227128	4.424534
N	-7.736924	1.338703	5.526027
N	-7.443045	-0.828805	5.028563
N	-10.094325	0.903967	5.085140
N	-9.835971	-1.314440	5.195074
O	-5.592033	4.101442	-3.417361
O	-6.197868	5.368107	0.409479
O	-6.102934	4.270077	3.733630
O	-5.814913	0.715848	4.387281
O	-11.765756	3.514627	-3.404821
O	-12.292701	5.352822	-0.192133
O	-11.669849	-0.462406	4.051749
C	-10.015429	-4.072409	3.078743
C	-8.084401	-3.958373	4.417028
C	-7.911613	-5.091325	3.359975
C	-6.072251	-3.632232	3.238278
C	-9.482320	-5.902277	1.543671
C	-5.870083	-5.762151	1.986119
C	-9.351166	-5.645702	-0.890072
C	-7.461811	-6.596507	0.161346
C	-7.284586	-6.658429	-1.392907
C	-5.476289	-5.470659	-0.437702
C	-9.001996	-6.279698	-3.250966
C	-5.518162	-5.623258	-2.905441
C	-9.476212	-4.265849	-4.600320
C	-7.262306	-5.084560	-4.693816
C	-7.397217	-3.838690	-5.631893
C	-5.673542	-3.457851	-4.066935
C	-9.450039	-2.467831	-6.277674
C	-5.889808	-1.795907	-5.872840
C	-9.925583	-0.195637	-5.399623
C	-7.923787	-0.450057	-6.593689
C	-8.231040	1.068562	-6.436850
C	-6.168691	0.598829	-5.422413
C	-6.585823	-2.000124	4.988743
C	-10.191448	-2.712808	5.130084
N	-9.426983	-3.495877	4.195347
N	-9.065808	-4.906639	2.500647
N	-7.019634	-3.026648	4.071076
N	-6.628150	-4.812120	2.769518
N	-8.718351	-5.891740	0.319433
N	-8.517079	-6.105783	-1.899828
N	-6.283074	-5.888306	0.608044
N	-6.105448	-5.850573	-1.613978
N	-8.598245	-5.247952	-4.175264
N	-8.756428	-3.389693	-5.404972
N	-6.249075	-4.678333	-3.733817
N	-6.365936	-2.948832	-5.152835
N	-9.113052	-1.078127	-6.089867
N	-9.381386	1.081191	-5.538311
N	-6.735742	-0.624667	-5.769030
N	-7.013704	1.592187	-5.880514
O	-11.155063	-3.899591	2.696505
O	-10.446637	-5.141275	-1.042950
O	-10.658187	-4.182437	-4.328235
O	-10.942392	-0.488504	-4.795025
O	-4.954960	-3.218049	3.004294
O	-4.400704	-4.910757	-0.344547
O	-4.714871	-2.941708	-3.522077
O	-5.106537	0.761406	-4.848312
H	-8.930984	4.556041	-6.039100
H	-8.803310	6.373981	-4.398291
H	-6.165573	5.849321	-1.924682
H	-7.235975	7.116931	-2.605674
H	-11.868542	5.803205	-2.520559
H	-10.735886	7.086240	-3.051133
H	-9.060948	7.867525	-1.232761
H	-9.466637	7.978867	1.178782
H	-6.538967	6.358559	2.641469
H	-7.913845	7.418713	3.086612
H	-12.176838	5.759387	2.148269
H	-11.146262	7.063529	2.813774
H	-9.587411	6.326107	4.666256
H	-9.646719	4.324119	6.079315
H	-6.301592	2.803942	5.620968
H	-7.618836	2.940288	6.828431
H	-11.858061	1.848049	4.624419
H	-11.109905	2.371336	6.166721
H	-9.202448	1.038137	6.993059
H	-8.488091	-1.306953	6.798071
H	-11.204602	1.914183	-5.034109
H	-10.403906	2.652048	-6.451924
H	-5.599686	3.049930	-5.599457
H	-6.831455	3.411355	-6.849706
H	-7.964526	-4.304978	5.453595
H	-7.917264	-6.100907	3.795076

H	-10.521235	-5.684102	1.288934
H	-9.413721	-6.903683	1.995990
H	-4.833743	-5.419228	1.976273
H	-5.934296	-6.745950	2.469769
H	-7.516738	-7.584501	0.637306
H	-7.135615	-7.675012	-1.779735
H	-10.092728	-6.257986	-3.221836
H	-8.658320	-7.252453	-3.622038
H	-4.521018	-5.214788	-2.731484
H	-5.439163	-6.573974	-3.450223
H	-6.940335	-5.994346	-5.216634
H	-7.241303	-4.070308	-6.694104
H	-10.515262	-2.580796	-6.069834
H	-9.246741	-2.728453	-7.324959
H	-4.920056	-1.527655	-5.450254
H	-5.772693	-2.065681	-6.933026
H	-7.728028	-0.759983	-7.628409
H	-8.475227	1.571142	-7.381565
H	-5.595323	-1.677773	4.665096
H	-6.518582	-2.418161	6.006951
H	-11.234830	-2.767831	4.815395
H	-10.082769	-3.142265	6.134689
C	-12.569973	1.482919	-1.102573
C	-11.732253	0.822849	-2.003680
C	-12.028739	2.334554	-0.140815
C	-10.358687	0.970080	-1.904856
H	-12.137275	0.196984	-2.787889
C	-10.652279	2.503950	-0.051419
H	-12.662987	2.895847	0.531667
C	-9.786470	1.791693	-0.908289
H	-9.726076	0.440807	-2.605783
H	-10.269961	3.222632	0.657943
C	12.418091	-0.032182	0.386618
C	11.500915	-0.934899	0.929896
C	12.085726	0.694270	-0.752936
C	10.241443	-1.067057	0.368476
H	11.763361	-1.551138	1.781289
C	10.841962	0.526552	-1.353673
H	12.794507	1.372469	-1.207069
H	9.534394	-1.751246	0.824663
H	10.656956	1.037591	-2.285903
C	9.878576	-0.330942	-0.783450
C	8.547109	-0.531535	-1.334987
S	7.615610	-1.924634	-0.888789

Supplementary References

1. Y. Inoue, K. Yamamoto, T. Wada, S. Everitt, X.-M. Gao, Z.-J. Hou, L.-H. Tong, S.-K. Jiang and H.-M. Wu, *J. Chem. Soc., Perkin Trans.* 1998, **2**, 1807–1816.
2. P. Thordarson, *Chem. Soc. Rev.,* 2011, **40**, 1305–1323.
3. H. Bakirci, X. Zhang and W. M. Nau, *J. Org. Chem.,* 2005, **70**, 39–46.
4. S. Fredrich, R. Gçstl, M. Herder, L. Grubert and S. Hecht, *Angew. Chem. Int. Ed.,* 2016, **55**, 1208 –1212.
5. M. Irie, T. Lifka, S. Kobatake and N. Kato, *J. Am. Chem. Soc.,* 2000, **122**, 4871–4876.
6. Z. Li, C. Zhang, Y. Ren, J. Yin and S. H. Liu, *Org. Lett.,* 2011, **13**, 6022-6025.
7. G. Liu, X. Xu, Y. Chen, X. Wu, H. Wu and Y. Liu, *Chem. Commun.,* 2016, **52**, 7966-

7969.

8. G. Liu, J. Zhu, Y. Zhou, Z. Dong, X. Xu and P. Mao, *Org. Lett.,* 2018, **20**, 5626−5630.

9. J. R. Lakowicz, Principles of Fluorescence Spectroscopy, 2nd Ed, Kluwer Academic/Plenum Publishers, 1999.

10. Q. Li, Y. He, J. Chang, L. Wang, H. Chen, Y.-W. Tan, H. Wang and Z. Shao, *J. Am. Chem. Soc.,* 2013, **135**, 14924−14927.

11. A. D. Becke, *Phys. Rev. A,* 1988, **38**, 3098–3100.

12. C. Lee, W. Yang and R. G. Parr, *Phys. Rev. B,* 1988, **37**, 785–789.

13. A. D. Becke, *J. Chem. Phys.,* 1993, **98**, 5648–5652.

14. A. D. Becke, *J. Chem. Phys.,* 1993, **98**, 1372–1377.

15. P. J. Stephens, F. J. Devlin, M. J. Frisch and C. F. Chabalowski, *J. Phys. Chem.,* 1994, **98**, 11623–11627.

16. S. Grimme, S. Ehrlich and L. Goerigk, *J. Comput. Chem.,* 2011, **32**, 1456−1465.

17. M. J. Frisch, G. W. Trucks, H. B. Schlegel, G. E. Scuseria, M. A. Robb, J. R. Cheeseman, G. Scalmani, V. Barone, B. Mennucci, G. A. Petersson, H. Nakatsuji, M. Caricato, X. Li, H. P. Hratchian, A. F. Izmaylov, J. Bloino, G. Zheng, J. L. Sonnenberg, M. Hada, M. Ehara, K. Toyota, R. Fukuda, J. Hasegawa, M. Ishida, T. Nakajima, Y. Honda, O. Kitao, H. Nakai, T. Vreven, J. A. Montgomery, Jr., J. E. Peralta, F. Ogliaro, M. Bearpark, J. J. Heyd, E. Brothers, K. N. Kudin, V. N. Staroverov, T. Keith, R. Kobayashi, J. Normand, K. Raghavachari, A. Rendell, J. C. Burant, S. S. Iyengar, J. Tomasi, M. Cossi, N. Rega, J. M. Millam, M. Klene, J. E. Knox, J. B. Cross, V. Bakken, C. Adamo, J. Jaramillo, R. Gomperts, R. E. Stratmann, O. Yazyev, A. J. Austin, R. Cammi, C. Pomelli, J. W. Ochterski, R. L. Martin, K. Morokuma, V. G. Zakrzewski, G. A. Voth, P. Salvador, J. J.

Dannenberg, S. Dapprich, A. D. Daniels, O. Farkas, J. B. Foresman, J. V. Ortiz, J. Cioslowski, and D. J. Fox, Gaussian 09, Revision E.01., Gaussian, Inc., Wallingford CT, 2013.

18. C. Y. Legault, ***CYLview, 1.0b;*** Université de Sherbrooke, 2009 (http://www.cylview.org).